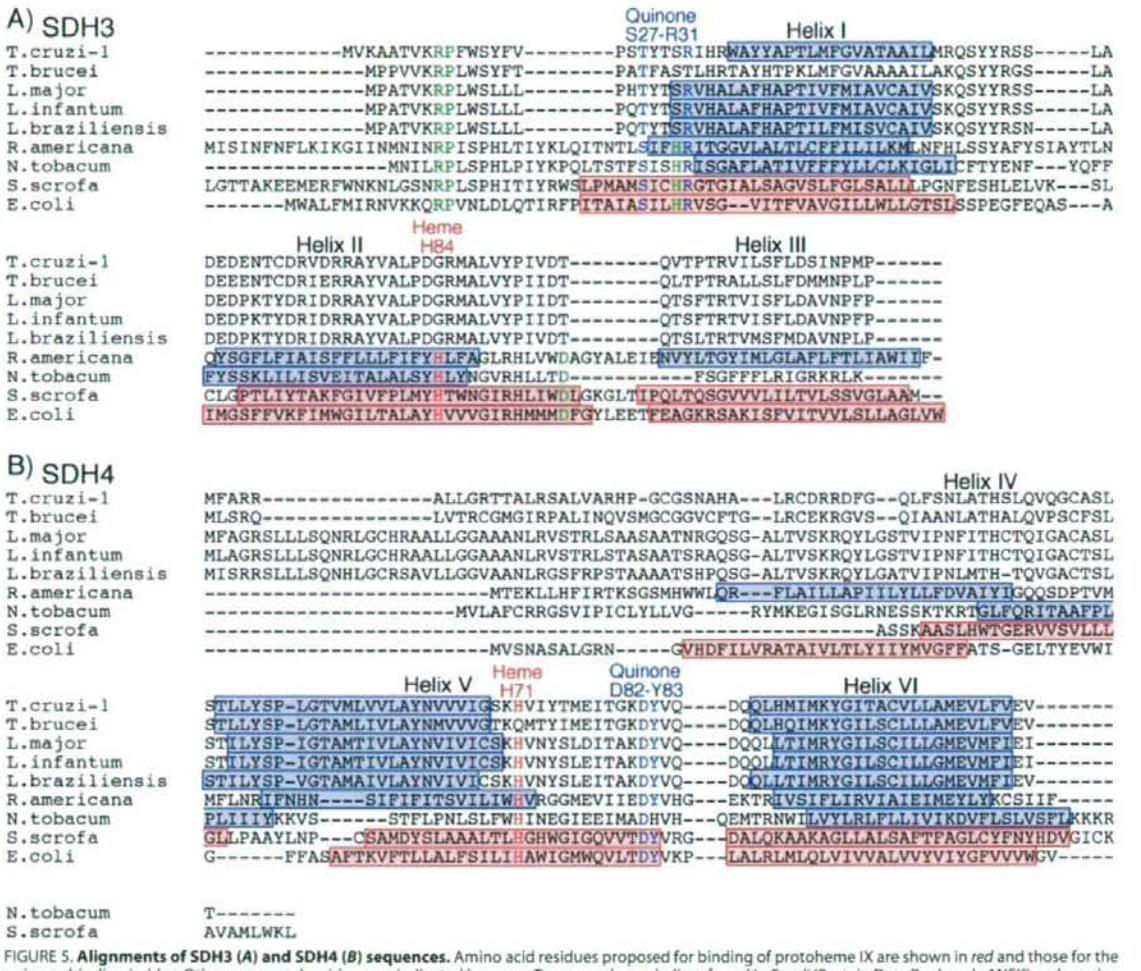

FIGURE 5. **Alignments of SDH3 (*A*) and SDH4 (*B*) sequences.** Amino acid residues proposed for binding of protoheme IX are shown in *red* and those for the quinone binding in *blue*. Other conserved residues are indicated by *green*. Transmembrane helices found in *E. coli* (Protein Data Bank code 1NEK) and porcine (Protein Data Bank code 1ZOY) Complex II are shown by *red rectangles*, and transmembrane helices predicted by TMHMM are indicated by *blue rectangles*. TMHMM failed to predict transmembrane helices in *T. brucei* SDH3. Residue numbers refer to *E. coli* SDH3 (SdhC) and SDH4 (SdhD). GenBank™ accession numbers for SDH3 and SDH4 sequences used are *T. cruzi* (XP_809410, XP_808211), *T. brucei* (XP_845531, XP_823384), *L. major* (XP_001684890, XP_001685874), *L. infantum* (XP_001467132), *L. brasiliensis* (XP_001566908, XP_001567905), *R. americana* (NP_044796, NP_044797), *Nicotiana tobacum* (YP_173376, YP_173457), *Sus scrofa* (1ZOY_C, 1ZOY_D), and *E. coli* (NP_415249, NP_415250).

and co-eluted with proteins and *b*-type cytochrome(s) at the second Superdex 200 chromatography (Fig. 2). Specific activity was increased 34-fold to 2.9 units/mg proteins, and the yield was ~2%. A hrCNE of the pure protein identified *T. cruzi* Complex II as an ~550-kDa complex (Fig. 3, *lanes 1* and *3*), which is 4-fold larger than bovine and yeast Complex II (130 kDa) and potato Complex II (150 kDa) (26, 27). Upon phase partitioning of the mitochondrial fraction with Triton X-114, the Complex II of *T. cruzi* was found only in the detergent-rich fraction (data not shown). Analysis of the detergent-rich fraction by hrCNE showed the Complex II as a single band at the same position as the pure enzyme (~550 kDa) (Fig. 3, *lanes 2* and *4*). These results indicated that the purified Complex II was obtained in its intact form. Interestingly, second dimensional analysis of both the purified Complex II and the detergent-rich fraction from phase partitioning with Triton X-114 with SDH activity showed that *T. cruzi* Complex II is composed of 12 subunits (Fig. 3, *lanes 5* and *6*). The same subunit composition was obtained by immunoaffinity purification of the partially purified enzyme (data not shown). The apparent molecular weight of the subunits ranges from 7.3 to 63 kDa (Fig. 3, *lanes 7* and *8*). Assuming the presence of equimolar amounts of subunits, a total molecular mass of Complex II would be 286.5 kDa, indicating that *T. cruzi* Complex II is a homodimer.

Identification of Genes Coded for Subunits—We determined N-terminal sequences (or internal peptide sequences in case of $SDH2_N$ and SDH8) of all subunits and identified genes coded for SDH1-1, $SDH2_N$, $SDH2_C$, SDH5–SDH7 (hydrophilic sub-

units), SDH3, SDH4, and SDH8–SDH11 (hydrophobic subunits) (Table 2). All subunits, except SDH1-1, are trypanosomatid-specific and structurally unrelated to plant-specific soluble subunits (AtSDH5–AtSDH8, 5–18 kDa) (27–29). All genes (except SDH6 with four copies) are present as two copies, which are assigned to either Esmeraldo or non-Esmeraldo haplotype (haploid genotype) in *T. cruzi* subgroup IIe. In contrast, only one copy each of the orthologues is present in *T. brucei*, *Leishmania major*, *Leishmania infantum*, and *Leishmania braziliensis* (supplemental Table S1). N-terminal sequence analysis of SDH3 and SDH7 showed that yields of two isoforms are similar (*i.e.* SDH3-1:SDH3-2 = 63:37, and SDH7-1:SDH7-2 = 54:46), indicating that isoforms are expressed from each haplotype. Because truncated isoforms for SDH1 and SDH5 in the Esmeraldo haplotype (see below) are not assembled into the 12-subunit complex and $SDH2_N$ and SDH9 isoforms have the identical sequence, 512 ($= 1^4 \times 4^1 \times 2^{(12-5)}$) kinds of heterogeneity may exist in the *T. cruzi* Complex II monomer (Table 2).

Flavoprotein Subunit—SDH1-1 (63-kDa band in Tricine-PAGE) cross-reacted with the antiserum against bovine SDH1 (data not shown) and is highly homologous to counterparts in *T. brucei* (93% identity), *L. major* (90%), *Homo sapiens* (59%), *Arabidopsis thaliana* (62%), *Saccharomyces cerevisiae* (61%), and *Escherichia coli* (48%, SdhA). Amino acid residues proposed for dicarboxylate binding and a FAD ligand histidine (12–14) are all conserved in SDH1-1. SDH1-1 and SDH5-1 of the non-Esmeraldo haplotype share a weak sequence similarity in the entire region, but the latter lacks amino acid residues responsible for FAD and dicarboxylate binding. In the Esmeraldo haplotype, SDH1-2 and SDH5-2 are truncated and contain only Met^1 to Gly^{167} of TcSDH1-1 and Ile^{305} to Met^{486} of TcSDH5-1, respectively (Table 2). These findings suggest that TcSDH1-1, TcSDH1-2, TcSDH5-1, and TcSDH5-2 might have evolved by gene duplication and subsequent degeneration.

Iron-Sulfur Subunit—Sequence analysis of the 25- and 21-kDa band proteins revealed that they contain the plant ferredoxin domain (Ip_N) and bacterial ferredoxin domain (Ip_C) of canonical SDH2 (Ip) in the N- and C-terminal half, respectively (Fig. 4). Sequence identities of Ip_N and Ip_C are 37 and 43%, respectively, to those of human SDH2 (Table 2), and the Ip_N and Ip_C domains contain all amino acid residues responsible for binding of iron-sulfur clusters and ubiquinone (12, 13, 30) (Fig. 4). Such a heterodimeric Ip subunit can be found in *T. brucei* (31), *T. cruzi*, *L. major*, *L. infantum*, and *L. braziliensis* (Tables 2), which belong to the order Trypanosomatida. Thus we named these subunits as $SDH2_N$ and $SDH2_C$, respectively.

Splitting of mitochondrial membrane proteins has been reported for cytochrome *c* oxidase CoxII in Apicomplexa and Chlorophyceae (32, 33), and ATP synthase α subunit in *Leishmania tarentolae* and *T. brucei* (34, 35). The former occurs at the gene level and the latter by post-translational cleavage. Sequence analysis indicates that heterodimeric SDH2 and CoxII have emerged from gene duplication followed by degeneration of the N- or C-terminal half of the duplication products. Conserved domains in degenerated duplicons, which have arisen from mitochondrion-to-nucleus transfer of the duplicated genes (32, 33, 36), must retain the potential for protein-protein interactions and constitute a heterodimeric functional subunit by trans-complementation.

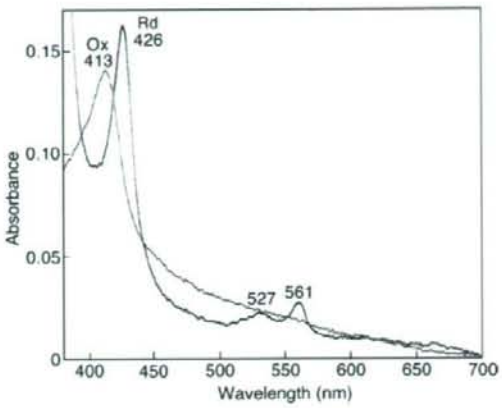

FIGURE 6. **Visible absorption spectra of *T. cruzi* Complex II.** Purified Complex II was desalted by ultrafiltration and diluted with 0.1 M sodium phosphate, pH 7.2, containing 0.1% SML at a final concentration of 0.06 mg/ml. Absorption spectra of the air-oxidized (*Ox, thin line*) and dithionite-reduced (*Rd, thick line*) forms were recorded at room temperature with UV-2400 spectrophotometer (Shimadzu Corp., Kyoto, Japan).

Membrane Anchor Subunits—Membrane anchor subunits in protist enzymes are highly divergent from bacterial and mammalian counterparts and difficult to find with conventional BLAST programs. We identified candidates for *T. cruzi* SDH3 and SDH4 by the presence of the quinone/heme-binding motifs "$RPX_{16}SX_2HR$ (SDH3 helix I)" and "$HX_{10}DY$ (SDH4 helix V)," respectively, present in membrane anchor subunits. In Complex II, Trp^{164} in SDH2 (Fig. 4) and Tyr^{83} in the SDH4 $HX_{10}DY$ motif (Fig. 5*B*) (*E. coli* numbering) could hydrogen bond to the O-1 atom of ubiquinone and contribute to the binding affinity (12, 37). Arg^{31} in the SDH3 SX_2HR motif (Fig. 5*A*) and Asp^{82} in the SDH4 $HX_{10}DY$ motif are in close proximity to ubiquinone and could interact with Tyr^{83} (37). Ser^{27} in the SDH3 SX_2HR motif has been shown to be essential for quinone binding (38) and is a candidate for hydrogen bonding to the O-4 atom of ubiquinone (30). The first arginine (Arg^9 in *E. coli* SDH3) in the $RPX_{16}SX_3R$ motif is in the vicinity of Glu^{186} in SDH1 and Asp^{106} in SDH2 and may play a structural role by making a hydrogen bond network.

In *T. cruzi*, SDH3 has the "$RPX_{11}SX_2HR$ motif in front of the predicted transmembrane helix I and lacks transmembrane helices II and III. However, sequence alignment suggests the presence of the alternative motif "$TX_2SR/(T)$" in the Trypanosomatida (Fig. 5*A*). In mitochondrial Complex II, protoheme IX is ligated by two His residues in the second transmembrane helix of SDH3 ("$HX_{10}D$" motif) and SDH4 ("$HX_{10}DY$" motif). A heme ligand in helix II (His^{84} in *E. coli* SDH3) may be substituted by a nearby histidine in the quinone-binding motif "SX_2HR" (39). In contrast, SDH4 lacks helix IV and appears to interact with heme and ubiquinone with the $HX_{10}DY$ motif. As in rice SDH4 (GenBank™ accession number NP_001045324), the heme ligand His is substituted by Gln in *T. brucei* SDH4. The presence of a bound heme or an alternative ligand in *T.*

brucei SDH4 needs to be tested in future studies. It is also possible that trypanosomatid-specific subunits could be assembled as a jigsaw puzzle-like membrane anchor.

Spectroscopic Properties of T. cruzi Complex II—Pyridine ferrohemochrome analysis showed that *T. cruzi* Complex II binds a stoichiometric amount of protoheme IX (0.85 heme/monomer of enzyme) indicating that monomer enzyme complex contains one heme. At room temperature, the air-oxidized and fully reduced forms of the purified enzyme showed peaks at 413 and 426, 527, and 561 nm, respectively (Fig. 6). Peak positions are similar to those reported for Complex II from *E. coli* (40), adult *A. suum* (41), and bovine (42, 43), where heme is ligated via histidine in the second helices of SDH3 and SDH4. Although heme has an important role in the assembly of Complex II, it is not essential for the reduction of ubiquinones (43, 44).

Enzymatic Properties of T. cruzi Complex II—We examined SQR activity of the purified enzyme and found the difference in apparent K_m values between Q_1 (33.9 ± 3.6 μM) and Q_2 (18.8 ± 6.4 μM) (Fig. 7), indicating that the 6-polyprenyl group of ubiquinone contributes to the binding affinity. The apparent V_{max} value of the *T. cruzi* Complex II was rather constant, 11.9 ± 2.2 for Q_1 and 11.5 ± 0.4 Q_2 units/mg proteins, respectively, and one-fourth of those reported for bovine and *E. coli* enzymes (45, 46). This is not surprising because *T. cruzi* complex II has about 2–3 times more proteins than the other enzymes. K_m values for ubiquinone and succinate (18.8 ± 6.4 μM (Q_2) and 1.48 ± 0.17 mM, respectively) were higher than 0.3 and 130 μM, respectively, of bovine enzyme (45), and 2 and 277 μM, respectively, of the *E. coli* enzyme (46, 47). Notably, the K_m value for succinate was comparable with 610 μM in adult *A. suum* (10), which expresses the stage-specific Complex II as quinol:fumarate reductase under hypoxic habitats in host organisms.

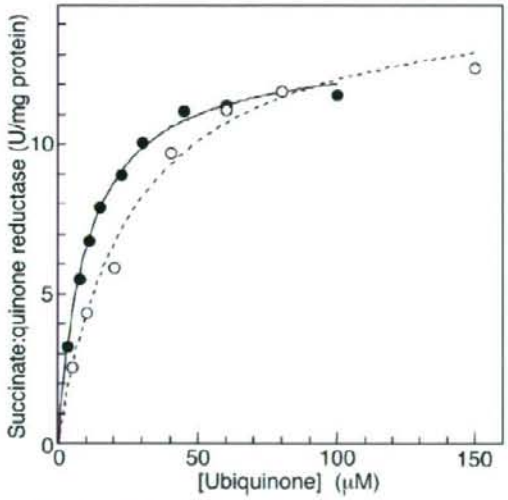

FIGURE 7. **Kinetic analysis of succinate-quinone reductase activity.** Succinate:ubiquinone reductase activity of the purified Complex II was determined with Q_1 (○) and Q_2 (●) at a protein concentration of 1.25 μg/ml in the presence of 10 mM sodium succinate. Data were fitted with the Michaelis-Menten equation using KaleidaGraph, and apparent K_m and V_{max} values were 30.3 ± 4.3 μM and 14.0 ± 1.2 units/mg protein, respectively, for Q_1 and 12.4 ± 0.7 μM and 11.9 ± 0.3 units/mg protein, respectively, for Q_2.

Then we examined effects of inhibitors for binding sites of quinones and dicarboxylates on SQR activity. Atpenin A5, a potent inhibitor for Complex II, inhibited the *T. cruzi* enzyme with the IC_{50} value of 6.4 ± 2.4 μM, which is 3 orders of magnitude higher than that of bovine Complex II (4 nM) (48). Furthermore, carboxin, 2-theonyltrifluoroacetone, plumbagin, and 2-heptyl-4-hydroxyquinoline *N*-oxide were ineffective (100 μM $< IC_{50}$). Structural divergence in trypanosomatid SDH3 and SDH4 could be the cause for lower binding affinities for both quinones and inhibitors. In addition, we found for the dicarboxylate-binding site that the IC_{50} value for malonate (40 μM) was much higher than the K_i value for bovine Complex II (1.3 μM) (45).

Structure of Trypanosomatid Complex II—To the best of our knowledge, this is the first report on the isolation of protist Complex II. *T. cruzi* Complex II has unusual subunit organization with six each of hydrophilic and hydrophobic subunits. Such a supramolecular structure and heterodimeric SDH2 ($SDH2_N$ and $SDH2_C$) are conserved in the Trypanosomatida. Furthermore, SDH1, $SDH2_N$, $SDH2_C$, SDH3, SDH4, and SDH8–SDH10 can be identified in the ongoing genome projects on the evolutionary relatives, the photosynthetic free-living *Euglena gracilis*, and the nonphotosynthetic euglenoid *Astasia longa* in the Euglenida. Thus a part of these features are common in the Euglenozoa, a divergent lineage of eukaryotes (Fig. 8).

Accumulation of noncatalytic subunits through expanding the protein interaction network could be a driving force for protein evolution. Structural and catalytic features are unique, and thus this enzyme could be a potential target for novel chemotherapeutic agents for trypanosomiasis and leishmaniasis.

Conclusion—The parasitic protist *T. brucei* is a gold mine where unprecedented biological phenomena like RNA editing and trans-splicing in mitochondria were originally discovered. It was found recently in *Diplonema papillatum*, a free-living evolutionary cousin,

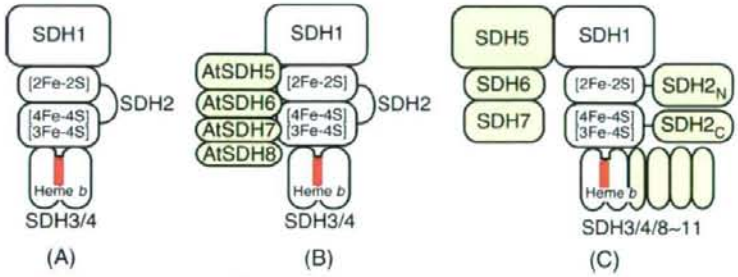

FIGURE 8. **Subunit organization of Complex II.** *A*, common four-subunit Complex II (*e.g.* mammals, *E. coli*); *B*, eight-subunit Complex II in plants (*e.g. A. thaliana*); and *C*, 12-subunit Complex II in the Trypanosomatida. Noncatalytic subunits and domains are shown in *yellow* and heme in *red*.

that mature mRNA for cytochrome *c* oxidase CoxI was assembled from nine gene fragments by a jigsaw puzzle mechanism (49). From a characterization of Complex II from *T. cruzi*, we revealed a novel supramolecular organization, which is conserved in the Trypanosomatida.

Parasites have exploited unique energy metabolic pathways as adaptations to their natural habitats within their hosts (50, 51). In fact, the respiratory systems of parasites typically show greater diversity in electron transfer pathways than those of host animals. As shown in this study, such is also the case with Complex II, which is a well known marker enzyme of mitochondria. Studies on the role of supramolecular Complex II in adaptation of trypanosomatids is now underway in our laboratory.

Acknowledgments—We thank Drs. J. L. Concepcion (Universidad de Los Andes, Merida-Venezuela) and T. Nara (Juntendo University) for kind advice; and Drs. M. Matsuzaki (University of Tokyo), T. Hashimoto (University of Tsukuba), G. Cecchini (University of California San Francisco), and M. Müller (Rockefeller University) for critical reading of the manuscript.

REFERENCES

1. World Health Organization (2007) *Report of the First Meeting of WHO Strategic and Technical Advisory Group on Neglected Tropical Diseases*, pp. 1–26, Geneva, Switzerland
2. Berriman, M., Ghedin, E., Hertz-Fowler, C., Blandin, G., Renauld, H., Bartholomeu, D. C., Lennard, N. J., Caler, E., Hamlin, N. E., Haas, B., Bohme, U., Hannick, L., Aslett, M. A., Shallom, J., Marcello, L., Hou, L., Wickstead, B., Alsmark, U. C., Arrowsmith, C., Atkin, R. J., Barron, A. J., Bringaud, F., Brooks, K., Carrington, M., Cherevach, I., Chillingworth, T. J., Churcher, C., Clark, L. N., Corton, C. H., Cronin, A., Davies, R. M., Doggett, J., Djikeng, A., Feldblyum, T., Field, M. C., Fraser, A., Goodhead, I., Hance, Z., Harper, D., Harris, B. R., Hauser, H., Hostetler, J., Ivens, A., Jagels, K., Johnson, D., Johnson, J., Jones, K., Kerhornou, A. X., Koo, H., Larke, N., Landfear, S., Larkin, C., Leech, V., Line, A., Lord, A., Macleod, A., Mooney, P. J., Moule, S., Martin, D. M., Morgan, G. W., Mungall, K., Norbertczak, H., Ormond, D., Pai, G., Peacock, C. S., Peterson, J., Quail, M. A., Rabbinowitsch, E., Rajandream, M. A., Reitter, C., Salzberg, S. L., Sanders, M., Schobel, S., Sharp, S., Simmonds, M., Simpson, A. J., Tallon, L., Turner, C. M., Tait, A., Tivey, A. R., Van Aken, S., Walker, D., Wanless, D., Wang, S., White, B., White, O., Whitehead, S., Woodward, J., Wortman, J., Adams, M. D., Embley, T. M., Gull, K., Ullu, E., Barry, J. D., Fairlamb, A. H., Opperdoes, F., Barrell, B. G., Donelson, J. E., Hall, N., Fraser, C. M., Melville, S. E., and El-Sayed, N. M. (2005) *Science* **309,** 416–422
3. Cazzulo, J. J. (1994) *J. Bioenerg. Biomembr.* **26,** 157–165
4. Besteiro, S., Barrett, M. P., Riviere, L., and Bringaud, F. (2005) *Trends Parasitol.* **21,** 185–191
5. Bringaud, F., Riviere, L., and Coustou, V. (2006) *Mol. Biochem. Parasitol.* **149,** 1–9
6. Takashima, E., Inaoka, D. K., Osanai, A., Nara, T., Odaka, M., Aoki, T., Inaka, K., Harada, S., and Kita, K. (2002) *Mol. Biochem. Parasitol.* **122,** 189–200
7. Van Hellemond, J. J., Opperdoes, F. R., and Tielens, A. G. (1998) *Proc. Natl. Acad. Sci. U. S. A.* **95,** 3036–3041
8. Harington, J. S. (1961) *Parasitology* **51,** 309–318
9. Roos, M. H., and Tielens, A. G. (1994) *Mol. Biochem. Parasitol.* **66,** 273–281
10. Saruta, F., Kuramochi, T., Nakamura, K., Takamiya, S., Yu, Y., Aoki, T., Sekimizu, K., Kojima, S., and Kita, K. (1995) *J. Biol. Chem.* **270,** 928–932
11. Cecchini, G. (2003) *Annu. Rev. Biochem.* **72,** 77–109
12. Yankovskaya, V., Horsefield, R., Tornroth, S., Luna-Chavez, C., Miyoshi, H., Leger, C., Byrne, B., Cecchini, G., and Iwata, S. (2003) *Science* **299,** 700–704
13. Sun, F., Huo, X., Zhai, Y., Wang, A., Xu, J., Su, D., Bartlam, M., and Rao, Z. (2005) *Cell* **121,** 1043–1057
14. Huang, L. S., Sun, G., Cobessi, D., Wang, A. C., Shen, J. T., Tung, E. Y., Anderson, V. E., and Berry, E. A. (2006) *J. Biol. Chem.* **281,** 5965–5972
15. El-Sayed, N. M., Myler, P. J., Bartholomeu, D. C., Nilsson, D., Aggarwal, G., Tran, A. N., Ghedin, E., Worthey, E. A., Delcher, A. L., Blandin, G., Westenberger, S. J., Caler, E., Cerqueira, G. C., Branche, C., Haas, B., Anupama, A., Arner, E., Aslund, L., Attipoe, P., Bontempi, E., Bringaud, F., Burton, P., Cadag, E., Campbell, D. A., Carrington, M., Crabtree, J., Darban, H., da Silveira, J. F., de Jong, P., Edwards, K., Englund, P. T., Fazelina, G., Feldblyum, T., Ferella, M., Frasch, A. C., Gull, K., Horn, D., Hou, L., Huang, Y., Kindlund, E., Klingbeil, M., Kluge, S., Koo, H., Lacerda, D., Levin, M. J., Lorenzi, H., Louie, T., Machado, C. R., McCulloch, R., McKenna, A., Mizuno, Y., Mottram, J. C., Nelson, S., Ochaya, S., Osoegawa, K., Pai, G., Parsons, M., Pentony, M., Pettersson, U., Pop, M., Ramirez, J. L., Rinta, J., Robertson, L., Salzberg, S. L., Sanchez, D. O., Seyler, A., Sharma, R., Shetty, J., Simpson, A. J., Sisk, E., Tammi, M. T., Tarleton, R., Teixeira, S., Van Aken, S., Vogt, C., Ward, P. N., Wickstead, B., Wortman, J., White, O., Fraser, C. M., Stuart, K. D., and Andersson, B. (2005) *Science* **309,** 409–415
16. Ivens, A. C., Peacock, C. S., Worthey, E. A., Murphy, L., Aggarwal, G., Berriman, M., Sisk, E., Rajandream, M. A., Adlem, E., Aert, R., Anupama, A., Apostolou, Z., Attipoe, P., Bason, N., Bauser, C., Beck, A., Beverley, S. M., Bianchettin, G., Borzym, K., Bothe, G., Bruschi, C. V., Collins, M., Cadag, E., Ciarloni, L., Clayton, C., Coulson, R. M., Cronin, A., Cruz, A. K., Davies, R. M., De Gaudenzi, J., Dobson, D. E., Duesterhoeft, A., Fazelina, G., Fosker, N., Frasch, A. C., Fraser, A., Fuchs, M., Gabel, C., Goble, A., Goffeau, A., Harris, D., Hertz-Fowler, C., Hilbert, H., Horn, D., Huang, Y., Klages, S., Knights, A., Kube, M., Larke, N., Litvin, L., Lord, A., Louie, T., Marra, M., Masuy, D., Matthews, K., Michaeli, S., Mottram, J. C., Muller-Auer, S., Munden, H., Nelson, S., Norbertczak, H., Oliver, K., O'Neil, S., Pentony, M., Pohl, T. M., Price, C., Purnelle, B., Quail, M. A., Rabbinowitsch, E., Reinhardt, R., Rieger, M., Rinta, J., Robben, J., Robertson, L., Ruiz, J. C., Rutter, S., Saunders, D., Schafer, M., Schein, J., Schwartz, D. C., Seeger, K., Seyler, A., Sharp, S., Shin, H., Sivam, D., Squares, R., Squares, S., Tosato, V., Vogt, C., Volckaert, G., Wambutt, R., Warren, T., Wedler, H., Woodward, J., Zhou, S., Zimmermann, W., Smith, D. F., Blackwell, J. M., Stuart, K. D., Barrell, B., and Myler, P. J. (2005) *Science* **309,** 436–442
17. Bourguignon, S. C., Mello, C. B., Santos, D. O., Gonzalez, M. S., and Souto-Padron, T. (2006) *Acta Trop.* **98,** 103–109
18. Concepcion, J. L., Chataing, B., and Dubourdieu, M. (1999) *Comp. Biochem. Physiol.* **122,** 211–222
19. Matsudaira, P. (1987) *J. Biol. Chem.* **262,** 10035–10038
20. Rosenfeld, J., Capdevielle, J., Guillemot, J. C., and Ferrara, P. (1992) *Anal. Biochem.* **203,** 173–179
21. Brusca, J. S., and Radolf, J. D. (1994) *Methods Enzymol.* **228,** 182–193
22. Wittig, I., Karas, M., and Schagger, H. (2007) *Mol. Cell. Proteomics* **6,** 1215–1225
23. Sabar, M., Balk, J., and Leaver, C. J. (2005) *Plant J.* **44,** 893–901
24. Berry, E. A., and Trumpower, B. L. (1987) *Anal. Biochem.* **161,** 1–15
25. Larkin, M. A., Blackshields, G., Brown, N. P., Chenna, R., McGettigan, P. A., McWilliam, H., Valentin, F., Wallace, I. M., Wilm, A., Lopez, R., Thompson, J. D., Gibson, T. J., and Higgins, D. G. (2007) *Bioinformatics (Oxf.)* **23,** 2947–2948
26. Schagger, H., and Pfeiffer, K. (2000) *EMBO J.* **19,** 1777–1783
27. Millar, A. H., Eubel, H., Jansch, L., Kruft, V., Heazlewood, J. L., and Braun, H. P. (2004) *Plant Mol. Biol.* **56,** 77–90
28. Eubel, H., Heinemeyer, J., and Braun, H. P. (2004) *Plant Physiol.* **134,** 1450–1459
29. Eubel, H., Heinemeyer, J., Sunderhaus, S., and Braun, H. P. (2004) *Plant Physiol. Biochem.* **42,** 937–942
30. Horsefield, R., Yankovskaya, V., Sexton, G., Whittingham, W., Shiomi, K., Omura, S., Byrne, B., Cecchini, G., and Iwata, S. (2006) *J. Biol. Chem.* **281,** 7309–7316
31. Allen, J. W., Ginger, M. L., and Ferguson, S. J. (2004) *Biochem. J.* **383,** 537–542
32. Funes, S., Davidson, E., Reyes-Prieto, A., Magallon, S., Herion, P., King, M. P., and Gonzalez-Halphen, D. (2002) *Science* **298,** 2155

33. Waller, R. F., and Keeling, P. J. (2006) *Gene (Amst.)* **383,** 33–37
34. Williams, N., and Frank, P. H. (1990) *Mol. Biochem. Parasitol.* **43,** 125–132
35. Nelson, R. E., Aphasizheva, I., Falick, A. M., Nebohacova, M., and Simpson, L. (2004) *Mol. Biochem. Parasitol.* **135,** 221–224
36. Adams, K. L., Rosenblueth, M., Qiu, Y. L., and Palmer, J. D. (2001) *Genetics* **158,** 1289–1300
37. Tran, Q. M., Rothery, R. A., Maklashina, E., Cecchini, G., and Weiner, J. H. (2006) *J. Biol. Chem.* **281,** 32310–32317
38. Yang, X., Yu, L., He, D., and Yu, C. A. (1998) *J. Biol. Chem.* **273,** 31916–31923
39. Maklashina, E., Rothery, R. A., Weiner, J. H., and Cecchini, G. (2001) *J. Biol. Chem.* **276,** 18968–18976
40. Kita, K., Vibat, C. R., Meinhardt, S., Guest, J. R., and Gennis, R. B. (1989) *J. Biol. Chem.* **264,** 2672–2677
41. Takamiya, S., Furushima, R., and Oya, H. (1986) *Biochim. Biophys. Acta* **848,** 99–107
42. Tushurashvili, P. R., Gavrikova, E. V., Ledenev, A. N., and Vinogradov, A. D. (1985) *Biochim. Biophys. Acta* **809,** 145–159
43. Tran, Q. M., Rothery, R. A., Maklashina, E., Cecchini, G., and Weiner, J. H. (2007) *Proc. Natl. Acad. Sci. U. S. A.* **104,** 18007–18012
44. Oyedotun, K. S., Sit, C. S., and Lemire, B. D. (2007) *Biochim. Biophys. Acta* **1767,** 1436–1445
45. Grivennikova, V. G., Gavrikova, E. V., Timoshin, A. A., and Vinogradov, A. D. (1993) *Biochim. Biophys. Acta* **1140,** 282–292
46. Maklashina, E., and Cecchini, G. (1999) *Arch. Biochem. Biophys.* **369,** 223–232
47. Miyadera, H., Hiraishi, A., Miyoshi, H., Sakamoto, K., Mineki, R., Murayama, K., Nagashima, K. V., Matsuura, K., Kojima, S., and Kita, K. (2003) *Eur. J. Biochem.* **270,** 1863–1874
48. Miyadera, H., Shiomi, K., Ui, H., Yamaguchi, Y., Masuma, R., Tomoda, H., Miyoshi, H., Osanai, A., Kita, K., and Omura, S. (2003) *Proc. Natl. Acad. Sci. U. S. A.* **100,** 473–477
49. Marande, W., and Burger, G. (2007) *Science* **318,** 415
50. Kita, K., and Takamiya, S. (2002) *Adv. Parasitol.* **51,** 95–131
51. Tielens, A. G., Rotte, C., van Hellemond, J. J., and Martin, W. (2002) *Trends Biochem. Sci.* **27,** 564–572
52. Krogh, A., Larsson, B., von Heijne, G., and Sonnhammer, E. L. L. (2001) *J. Mol. Biol.* **305,** 567–580
53. Mitaku, S., Hirokawa, T., and Tsuji, T. (2002) *Bioinformatics* **18,** 608–616

Cell Metabolism
Article

Fasting-Induced Hypothermia and Reduced Energy Production in Mice Lacking Acetyl-CoA Synthetase 2

Iori Sakakibara,[1,2] Takahiro Fujino,[3] Makoto Ishii,[2,4] Toshiya Tanaka,[1] Tatsuo Shimosawa,[5] Shinji Miura,[6] Wei Zhang,[7] Yuka Tokutake,[8] Joji Yamamoto,[2,9] Mutsumi Awano,[10] Satoshi Iwasaki,[1,2] Toshiyuki Motoike,[2,11] Masashi Okamura,[1,9] Takeshi Inagaki,[1] Kiyoshi Kita,[10] Osamu Ezaki,[6] Makoto Naito,[13] Tomoyuki Kuwaki,[7] Shigeru Chohnan,[8] Tokuo T. Yamamoto,[14] Robert E. Hammer,[12] Tatsuhiko Kodama,[1] Masashi Yanagisawa,[2,11] and Juro Sakai[1,2,*]

[1]Laboratory for Systems Biology and Medicine, Research Center for Advanced Science and Technology, University of Tokyo, Tokyo 153-8904, Japan
[2]ERATO, Japan Science and Technology Agency (JST), Tokyo 102-0075, Japan
[3]Department of Bioscience, Integrated Center for Sciences, Ehime University Graduate School of Medicine, Ehime 791-0295, Japan
[4]Department of Neurology, Weill Cornell Medical College of Cornell University, 525 East 68th Street, New York, NY 10021, USA
[5]Department of Clinical Laboratory, Faculty of Medicine, University of Tokyo, Tokyo 113-8655, Japan
[6]Nutritional Science Program, National Institute of Health and Nutrition, 1-23-1, Toyama, Shinjuku-ku, Tokyo 162-8636, Japan
[7]Departments of Molecular & Integrative Physiology and Autonomic Physiology, Graduate School of Medicine, Chiba University, Chiba, 260-8670, Japan
[8]Department of Bioresource Science, Ibaraki University College of Agriculture, 3-21-1 Chuo, Ami, Ibaraki 300-0393, Japan
[9]Division of Nephrology, Endocrinology, and Vascular Medicine, Department of Medicine, Tohoku University Graduate School of Medicine, Sendai 980-8574, Japan
[10]Department of Biomedical Chemistry, Graduate School of Medicine, University of Tokyo, Bunkyo-ku, Tokyo 113-0033, Japan
[11]Howard Hughes Medical Institute, Department of Molecular Genetics
[12]Department of Biochemistry
University of Texas Southwestern Medical Center, Dallas, TX 75390, USA
[13]Department of Cellular Function, Division of Cellular and Molecular Pathology, Niigata University Graduate School of Medical and Dental Sciences, Niigata 951-8510, Japan
[14]Center for Advanced Genome Research, Institute of Development, Aging, and Cancer, Tohoku University, Sendai 981-8555, Japan
*Correspondence: jmsakai-tky@umin.ac.jp
DOI 10.1016/j.cmet.2008.12.008

SUMMARY

Acetate is activated to acetyl-CoA by acetyl-CoA synthetase 2 (AceCS2), a mitochondrial enzyme. Here, we report that the activation of acetate by AceCS2 has a specific and unique role in thermogenesis during fasting. In the skeletal muscle of fasted *AceCS2*$^{-/-}$ mice, ATP levels were reduced by 50% compared to *AceCS2*$^{+/+}$ mice. Fasted *AceCS2*$^{-/-}$ mice were significantly hypothermic and had reduced exercise capacity. Furthermore, when fed a low-carbohydrate diet, 4-week-old weaned *AceCS2*$^{-/-}$ mice also exhibited hypothermia accompanied by sustained hypoglycemia that led to a 50% mortality. Therefore, AceCS2 plays a significant role in acetate oxidation needed to generate ATP and heat. Furthermore, *AceCS2*$^{-/-}$ mice exhibited increased oxygen consumption and reduced weight gain on a low-carbohydrate diet. Our findings demonstrate that activation of acetate by AceCS2 plays a pivotal role in thermogenesis, especially under low-glucose or ketogenic conditions, and is crucially required for survival.

INTRODUCTION

Mammals have evolved complex metabolic systems to survive extended periods of nutrient deprivation. Under a fed condition, mammals utilize glucose as the main metabolic fuel. Under ketogenic conditions such as fasting, low-carbohydrate diet feeding, and diabetes, fatty acids and ketone bodies are utilized as the main energy sources. Ketone bodies, utilized mainly in brain and also some in skeletal muscle and heart (Fukao et al., 2004), are produced in liver from acetyl-CoA released after β oxidation of fatty acids in mitochondria. Several lines of evidence report that acetate is synthesized in the liver and utilized as an alternative fuel under ketogenic conditions. For instance, acetate concentration in livers of starved rats is quite high (Murthy and Steiner, 1973). Also, formation of free acetate by the liver has been reported from studies utilizing isolated rat liver perfusion and studies using isolated hepatocytes (Leighton et al., 1989; Seufert et al., 1974; Yamashita et al., 2001). Acetate is generated following hydrolysis of acetyl-CoA by acetyl CoA hydrolase, an end product of fatty acid oxidation in rat liver peroxisomes (Leighton et al., 1989). However, it is not known whether acetate is actually utilized as an alternative fuel (substituting for glucose, fatty acids, or ketone bodies) in peripheral tissues such as skeletal muscle, heart, brown adipose tissues (BAT), or brain.

Acetyl-CoA synthetase (AceCS, EC 6.2.1.1) ligates acetate and CoA to generate acetyl-CoA. In mammals, there are two AceCSs with similar enzymatic properties: one, designated AceCS1, is a cytosolic enzyme, whereas AceCS2 is an enzyme of the mitochondrial matrix (Fujino et al., 2001; Luong et al., 2000). AceCS1 and AceCS2 are regulated posttranscriptionally by members of the sirtuin family of deacetylases, SIRT1 and SIRT3, respectively. Both SIRT1 and SIRT3 are upregulated during caloric restriction and have been implicated as mediating

the longevity-promoting effects of caloric restriction (Schwer and Verdin, 2008; Yang et al., 2007).

AceCS1 provides acetyl-CoA for the synthesis of fatty acids and cholesterol. AceCS1 is highly expressed in liver, and its transcription is regulated by sterol regulatory element-binding proteins (SREBPs), basic helix-loop-helix leucine zipper transcription factors that activate multiple genes involved in cholesterol and fatty acid metabolism (Ikeda et al., 2001; Luong et al., 2000). By contrast, AceCS2 produces acetyl-CoA for oxidation through the tricarboxylic acid cycle to produce ATP and CO_2 (Fujino et al., 2001). AceCS2 is highly expressed in BAT, heart, and skeletal muscle. Importantly, the levels of its mRNAs in BAT, heart, and skeletal muscle are robustly increased under ketogenic conditions, whereas the level of its mRNAs in liver was barely detectable (Fujino et al., 2001). The fasting-induced transcriptional activation of AceCS2 in the skeletal muscle is largely controlled by Krüppel-like factor 15 (KLF15), a member of the Krüppel-like family of transcription factors (Yamamoto et al., 2004) that regulates many genes involved in gluconeogenesis such as phosphoenolpyruvate carboxykinase (PEPCK) and amino acid-degrading enzymes required under ketogenic conditions (Gray et al., 2007; Teshigawara et al., 2005).

To examine whether acetate is utilized as a fuel under ketogenic conditions, we generated *AceCS2*-deficient mice. In this paper, we show that AceCS2 is essential for energy expenditure under ketogenic conditions.

RESULTS

Generation of *AceCS2*-Deficient Mice

To evaluate the role of AceCS2 in vivo, we generated mice lacking *AceCS2*. We constructed an insertion-type vector that disrupts exon 1 of the mouse *AceCS2* gene (Figure 1A). Two lines of mice harboring insertions in *AceCS2* were identified by Southern blotting (Figure 1B). Genotyping was performed by PCR (Figure 1C), and the absence of AceCS2 transcripts (Figure 1D) and protein (Figure 1E) was confirmed by quantitative real-time PCR (QRT-PCR) and immunoblot analysis, respectively. Wild-type (*AceCS2*$^{+/+}$), heterozygous (*AceCS2*$^{+/-}$), and homozygous (*AceCS2*$^{-/-}$) mice were born at frequencies predicted by simple Mendelian ratios. *AceCS2*$^{-/-}$ mice of both sexes were normally fertile and typical in appearance. No histological abnormalities were seen following light microscopy of sections obtained from multiple tissues of adult male mice, including bone, brain, stomach, heart, intestine, kidney, liver, pancreas, white adipose tissue, BAT, and skeletal muscle (data not shown). At birth, the body weight and length of *AceCS2*$^{-/-}$ mice were indistinguishable from their littermates. By the time of weaning (4 weeks of age), both male and female *AceCS2*$^{-/-}$ mice exhibited significant growth retardation (Figures S1A–S1C available online). After weaning, *AceCS2*$^{-/-}$ mice fed on normal chow diet began to catch up with *AceCS2*$^{+/+}$ mice in both body weight and body length. By 20 weeks of age, the body weight of the *AceCS2*$^{-/-}$ mice became comparable to their littermates (Figures S1A and S1B). Food intake of 4-week-old *AceCS2*$^{-/-}$ mice was slightly decreased compared to *AceCS2*$^{+/+}$ mice but became comparable to that of their littermates by 20 weeks of age (Figure S1D). Plasma parameters of *AceCS2*$^{+/+}$ and *AceCS2*$^{-/-}$ mice before weaning (2–4 weeks of age) and at 26 weeks of age are shown in Table S1. Glucose, ketone bodies, nonesterified fatty acids (NEFA), and insulin levels were indistinguishable between *AceCS2*$^{+/+}$ and *AceCS2*$^{-/-}$ mice at both 2–4 weeks of age and at 26 weeks of age (Table S1). Plasma concentration of growth hormone and

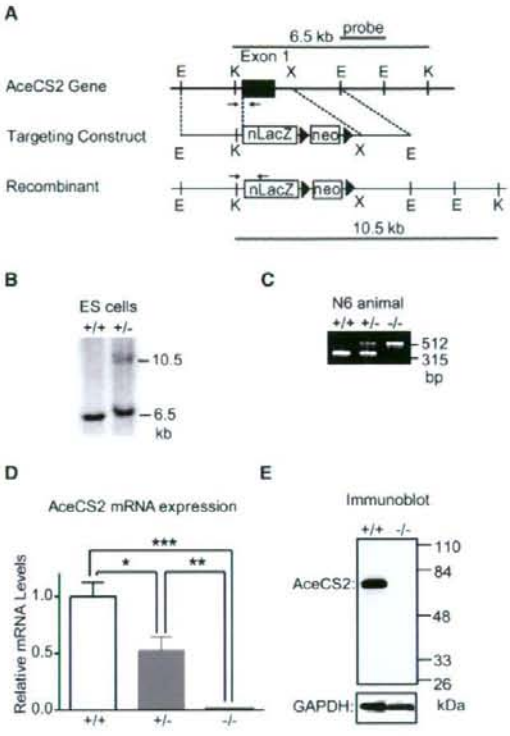

Figure 1. Generation of *AceCS2*-Deficient Mice

(A) Diagram of the targeting strategy. Only the relevant restriction sites are indicated. Locations of the probes for Southern blot analysis (bars) and PCR primers (arrows) for genotyping are shown.

(B) Southern blot analysis of KpnI-digested DNA from ES cell clones. Southern blotting was performed with the probe indicated in (A). KpnI digestion resulted in a 6.5 kb fragment in wild-type DNA and a 10.5 kb fragment in homologous recombinants.

(C) An ethidium bromide-stained agarose gel illustrates PCR products for genotyping *AceCS2*$^{+/+}$, *AceCS2*$^{+/-}$, and *AceCS2*$^{-/-}$ mice. A description of the PCR genotyping strategy is contained in the Experimental Procedures.

(D) QRT-PCR analysis of AceCS2 transcripts. Total RNA from heart of *AceCS2*$^{+/+}$, *AceCS2*$^{+/-}$, and *AceCS2*$^{-/-}$ mice were analyzed by QRT-PCR quantification as described in the Experimental Procedures. β-actin was used as the invariant control. Values represent the amount of mRNA relative to that in *AceCS2*$^{+/+}$ mice, which is arbitrarily defined as 1. Data are mean ± SEM. *$p < 0.05$ compared to *AceCS2*$^{+/+}$; **$p < 0.01$ compared to *AceCS2*$^{+/-}$; ***$p < 0.001$ compared to *AceCS2*$^{+/+}$ ($^{+/+}$, n = 9; $^{+/-}$, n = 17; $^{-/-}$, n = 7).

(E) Immunoblot analysis, with an affinity-purified anti-rabbit polyclonal AceCS2 antibody, of *AceCS2*$^{+/+}$ and *AceCS2*$^{-/-}$ mouse heart protein. Each lane was loaded with 20 μg of whole-cell lysates in SDS lysis buffer from the hearts. GAPDH was detected with a polyclonal anti-GAPDH antibody as a loading control.

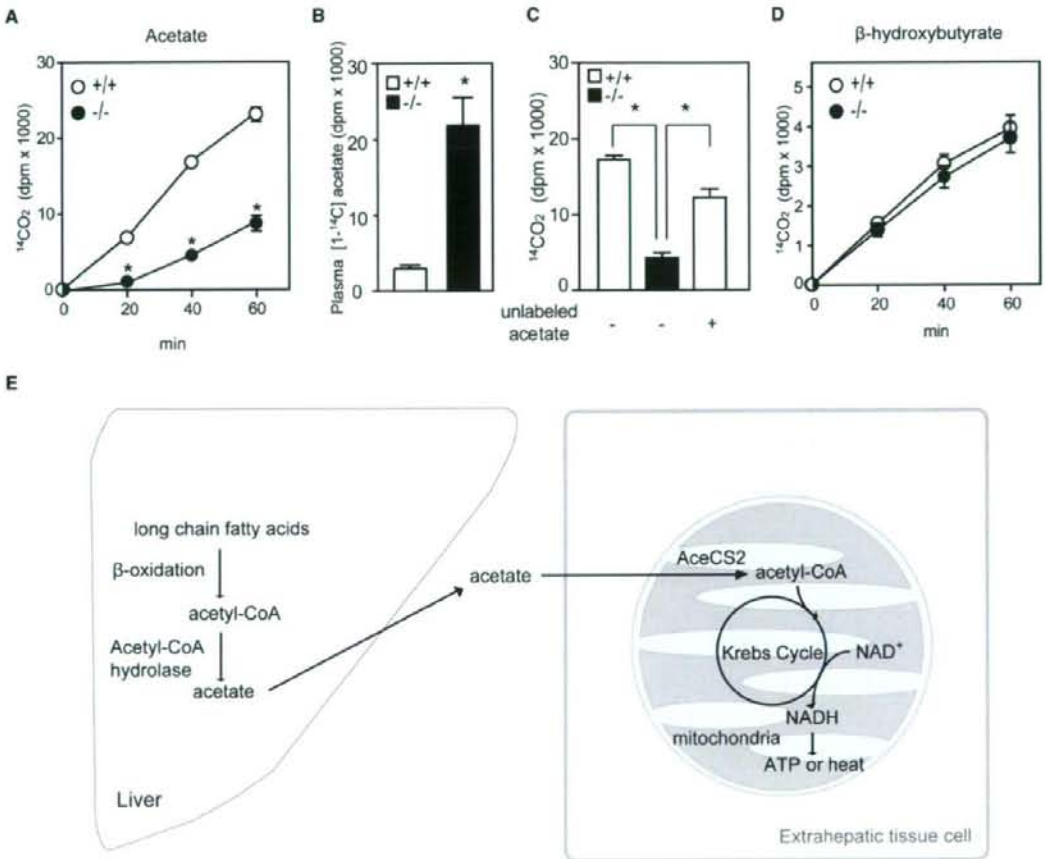

Figure 2. *AceCS2*$^{-/-}$ Mice Exhibit Lower Whole-Body Acetic Acid Oxidation during Fasting

After 48 hr of fasting, 12-week-old male mice were tested for their ability to oxidize [1-^{14}C]acetate or [1-^{14}C]β-hydroxybutyrate to $^{14}CO_2$ at 20, 40, and 60 min after intraperitoneal (i.p.) injection with the labeled compound.

(A) Rate of $^{14}CO_2$ production from acetate. *$p < 0.001$ compared to *AceCS2*$^{+/+}$.

(B) Total plasma [1-^{14}C]acetate was measured after 60 min.

(C) Rate of $^{14}CO_2$ production from acetate with inclusion of unlabeled acetate. Unlabeled acetate (0.6 g/kg) was injected with [1-^{14}C]acetate, and the acetate oxidation rate was measured after 40 min.

(D) Rate of $^{14}CO_2$ production from β-hydroxybutyrate (*AceCS2*$^{+/+}$, n = 6; *AceCS2*$^{-/-}$, n = 6).

(E) Model for the role of AceCS2 in energy metabolism.

(A–D) Data are mean ± SEM.

insulin-like growth factor-1 (IGF-1) of *AceCS2*$^{-/-}$ mice (2–4 weeks of age) were also comparable to *AceCS2*$^{+/+}$. The plasma leptin levels of 2- to 4-week-old *AceCS2*$^{-/-}$ mice were lower than those of age-matched, wild-type littermates. Notably, plasma acetate levels were markedly elevated in *AceCS2*$^{-/-}$ mice compared to *AceCS2*$^{+/+}$ mice (Table S1).

AceCS2$^{-/-}$ Mice Exhibited Marked Reduction in Whole-Body Acetate Oxidation

To examine whether acetate is, in fact, utilized as a fuel during fasting, we performed whole-body acetate oxidization assays. Mice were fasted for 48 hr and then injected with [^{14}C]acetate. Figure 2A shows the sharply decreased rate of acetate oxidation in *AceCS2*$^{-/-}$ mice. As a consequence, [^{14}C]acetate levels remained high in the plasma of *AceCS2*$^{-/-}$ mice, whereas *AceCS2*$^{+/+}$ mice showed very low levels of plasma [^{14}C]acetate (Figure 2B). Because higher levels of plasma acetate in *AceCS2*$^{-/-}$ mice might affect the acetate oxidation rate, we also examined the oxidation of [^{14}C]acetate with the inclusion of unlabeled acetate at similar levels to those found in the *AceCS2*$^{-/-}$ mice (about 2 mM) (Figure 2C). Injection of unlabeled acetate (0.6 mg/kg) led to rapid increase in plasma acetate to

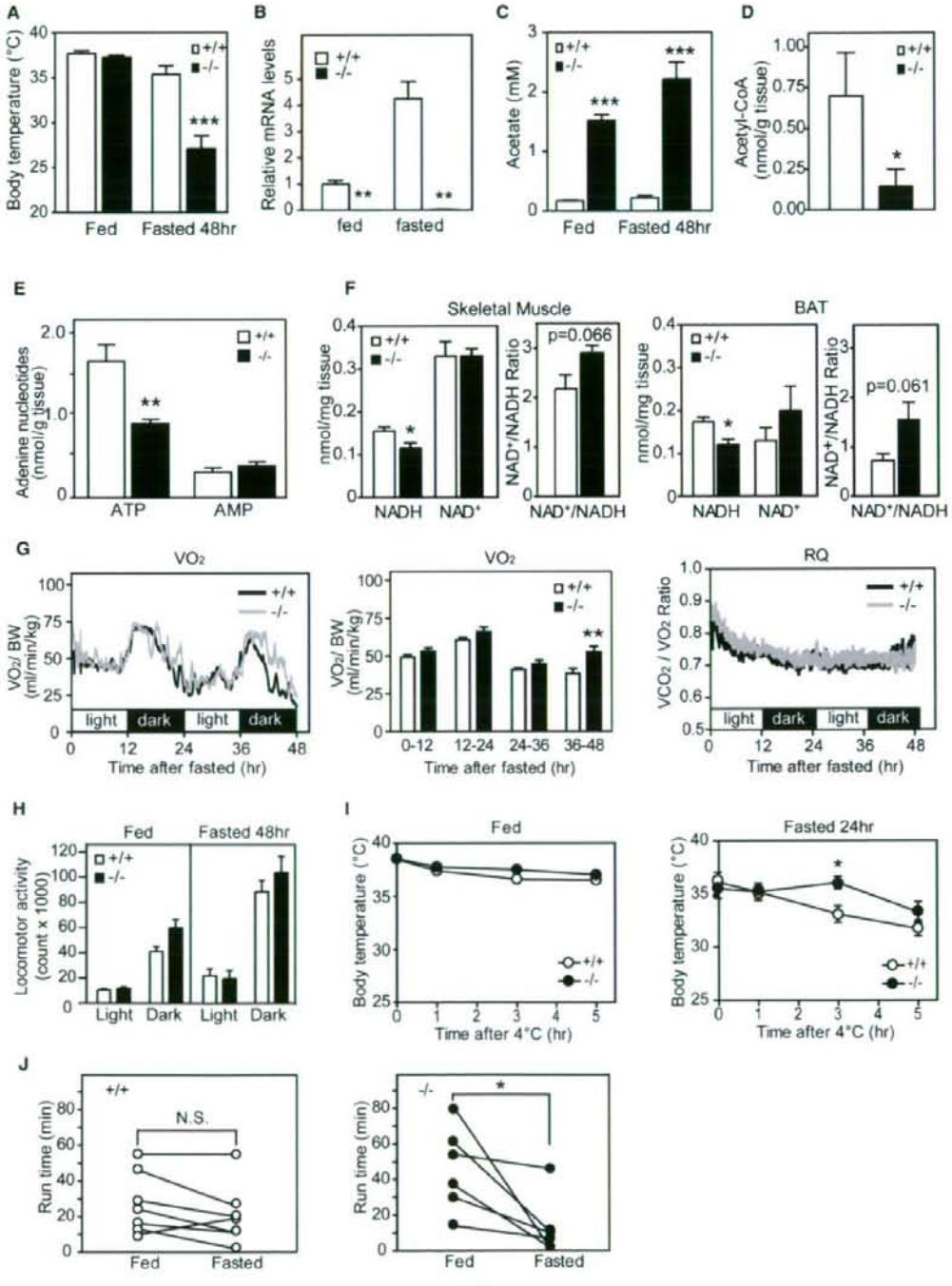
A
Body temperature (°C)
Fed
Fasted 48hr
B
Relative mRNA levels
fed
fasted
C
Acetate (mM)
Fed
Fasted 48hr
D
Acetyl-CoA (nmol/g tissue)
E
Adenine nucleotides (nmol/g tissue)
ATP
AMP
F
Skeletal Muscle
BAT
nmol/mg tissue
NAD+/NADH Ratio
p=0.066
p=0.061
NADH
NAD+
NAD+/NADH
G
VO2
VO2/ BW (ml/min/kg)
light
dark
Time after fasted (hr)
RQ
VCO2 / VO2 Ratio
0-12
12-24
24-36
36-48
H
Locomotor activity (count x 1000)
Light
Dark
I
Body temperature (°C)
Time after 4°C (hr)
Fasted 24hr
J
Run time (min)
N.S.

2 mM at 40 min after the injection (data not shown). Under this condition, the rate of acetate oxidation measured was still significantly lower in *AceCS2*$^{-/-}$ mice (Figure 2C). Oxidation of ketone bodies was similar, irrespective of genotype (Figure 2D), indicating that ketone body utilization is normal in *AceCS2*$^{-/-}$ mice.

Together with our previous report showing that [^{14}C]acetate is incorporated into CO_2 in AceCS2-transfected cells (Fujino et al., 2001), these data indicate that, in mice, acetate oxidation to form CO_2 and ATP requires AceCS2. Previous studies showed that an appreciable amount of acetate is generated in liver by hepatic acetyl-CoA hydrolase, a ubiquitous peroxisome enzyme, and that this acetate can subsequently be utilized by extrahepatic tissues (Leighton et al., 1989; Murthy and Steiner, 1973; Seufert et al., 1974). We propose a model in which acetate is generated in liver from fatty acids and released into the circulation under conditions when glucose is low, such as 48 hr fasting or low-carbohydrate/ high-fat diet. AceCS2 is necessary for salvaging this acetate for use in extrahepatic tissues such as skeletal muscle and BAT, where acetate is reactivated for reentry to the mitochondrial TCA cycle to generate ATP and heat (Figure 2E).

Adult *AceCS2*$^{-/-}$ Mice Exhibit Low Body Temperature and Reduced Capacity to Sustain Running Exercise under a Fasting Condition

To further evaluate the physiological role of acetate oxidation, 12-week-old *AceCS2*$^{-/-}$ mice were freely fed a standard rodent diet or fasted for 48 hr. During normal fed states, there was no significant difference in core temperature between *AceCS2*$^{+/+}$ and *AceCS2*$^{-/-}$ mice (Figure 3A). After 48 hr of fasting, *AceCS2*$^{+/+}$ mice were able to maintain their core body temperatures, but *AceCS2*$^{-/-}$ mice had significantly lower core body temperatures (Figure 3A). These data demonstrate that acetate activation by AceCS2 is important for maintenance of normal body temperature, likely as a result of heat production during fasting. Indeed, the mRNA levels in BAT of AceCS2 were 4-fold higher under the fasted condition than under the fed condition, suggesting that AceCS2 has an important role during fasting condition (Figure 3B).

In mice, BAT and skeletal muscle are the main thermogenic tissues in which oxidation of fatty acid, stimulated by the sympathetic nervous system, generates heat through uncoupling proteins (UCPs) present in mitochondria (Spiegelman and Flier, 2001). During fasting, the quantity and morphology of mitochondria in BAT and skeletal muscle are indistinguishable between *AceCS2*$^{+/+}$ mice and sex- and age-matched *AceCS2*$^{-/-}$ mice (Figure S2A). Oxidative proteins such as UCPs are thought to be important in thermogenesis (Matthias et al., 2000; Spiegelman and Flier, 2001). The mRNA levels of UCP1 in the BAT or UCP2 and UCP3 in the skeletal muscle did not differ significantly between *AceCS2*$^{+/+}$ and *AceCS2*$^{-/-}$ mice. Other thermogenic molecules PGC1α and PPARδ also did not differ in mRNA levels (Figure S2B and data not shown).

To evaluate substrate supply, we determined the levels of various metabolites in the plasma of fed and 48 hr fasted 12-week-old male *AceCS2*$^{+/+}$ and *AceCS2*$^{-/-}$ mice (Table S2). There was no significant change in plasma glucose or in NEFA and ketone body levels between *AceCS2*$^{+/+}$ and *AceCS2*$^{-/-}$ mice (Table S2). There was also no significant difference in the percentage of fat mass between fed *AceCS2*$^{-/-}$ and *AceCS2*$^{+/+}$ mice as assessed by dual-energy X-ray absorption (DEXA) (Table S2). However, plasma acetate was 5- to 10-fold higher in *AceCS2*$^{-/-}$ mice as compared to *AceCS2*$^{+/+}$ mice under both fed and fasted conditions (Figure 3C). These data indicate that acetate utilization is impaired in *AceCS2*$^{-/-}$ mice, implying that a deficit in extrahepatic acetate utilization causes fasting-induced hypothermia. Acetyl-CoA levels were decreased by 75% in fasted *AceCS2*$^{-/-}$ mice (Figure 3D). NADH and ATP levels in skeletal muscles of fasted *AceCS2*$^{-/-}$ mice were significantly reduced compared to those found in *AceCS2*$^{+/+}$ mice (Figures 3E and 3F). These data indicate that AceCS2 plays a pivotal role in supplying acetyl-CoA for ATP production during 48 hr of fasting. Oxygen consumption was significantly increased after 36 hr fasting, and locomotor activity was not reduced (Figures 3G and 3H).

The hypothermia in *AceCS2*$^{-/-}$ mice also differs from adaptive hypothermia in response to cold (Lowell and Spiegelman, 2000). Exposure of these *AceCS2*$^{-/-}$ mice to low temperature (4°C) did

Figure 3. *AceCS2*-Deficient Mice Exhibit Low Body Temperature and Reduced Exercise Capacity during Fasting

(A) Core temperature of male mice (12 weeks old) fed on normal chow diet was monitored after 48 hr fasting (*AceCS2*$^{+/+}$, n = 8; *AceCS2*$^{-/-}$, n = 7). *$p < 0.05$ compared to *AceCS2*$^{+/+}$.

(B) Relative mRNA expression levels of AceCS2 in BAT of male mice (12 weeks old, six to seven per genotype). **$p < 0.01$ compared to *AceCS2*$^{+/+}$.

(C) Plasma acetate levels of male mice (12 weeks old) fed or fasted for 48 hr (fed *AceCS2*$^{+/+}$, n = 4; fasted *AceCS2*$^{+/+}$, n = 4; fed *AceCS2*$^{-/-}$, n = 4; fasted *AceCS2*$^{-/-}$, n = 4).

(D) Acetyl-CoA levels in gastrocnemius muscle from 48 hr fasted male *AceCS2*$^{+/+}$ and *AceCS2*$^{-/-}$ mice (12 weeks old) were measured (*AceCS2*$^{+/+}$, n = 7; *AceCS2*$^{-/-}$, n = 8).

(E) ATP content is markedly reduced in *AceCS2*$^{-/-}$ mice. ATP and AMP contents of gastrocnemius muscle from male *AceCS2*$^{+/+}$ and *AceCS2*$^{-/-}$ mice were measured at 12 weeks of age (*AceCS2*$^{+/+}$, n = 7; *AceCS2*$^{-/-}$, n = 8). **$p < 0.01$ compared to *AceCS2*$^{+/+}$.

(F) NAD$^+$ and NADH levels and NAD$^+$/NADH ratio in gastrocnemius muscle and BAT of 48 hr fasted male *AceCS2*$^{+/+}$ and *AceCS2*$^{-/-}$ mice (12 weeks old) (*AceCS2*$^{+/+}$, n = 4; *AceCS2*$^{-/-}$, n = 4).

(G) Oxygen consumption (VO_2) (left panel), average of VO_2 (center panel), and RQ (respiratory quotient) (right panel) were determined in fasted male mice (12 weeks old) by indirect calorimetry (*AceCS2*$^{+/+}$, n = 6; *AceCS2*$^{-/-}$, n = 5).

(H) Total locomotor activity of male mice (14 weeks old) was measured by beam breaks in the light and dark periods (*AceCS2*$^{+/+}$, n = 12; *AceCS2*$^{-/-}$, n = 12).

(I) Male mice (12 weeks old) given food and water ad libitum were subjected to cold (4°C) (left panel) (*AceCS2*$^{+/+}$, n = 10; *AceCS2*$^{-/-}$, n = 11). Male mice (12 weeks old) fasted for 24 hr and given water ad libitum were subjected to cold (4°C) (right panel) (*AceCS2*$^{+/+}$, n = 7; *AceCS2*$^{-/-}$, n = 8). Core temperature was monitored over a 5 hr period.

(J) Male mice (12 weeks old, nine per genotype) were subjected to a run-to-exhaustion protocol on a motorized treadmill under fed conditions and 48 hr fasted conditions (*AceCS2*$^{+/+}$, n = 9; *AceCS2*$^{-/-}$, n = 9). *$p < 0.05$ compared to fed.

All values are mean ± SEM.

not further reduce their body temperatures under the fed condition (Figure 3I, left panel). We next examined the effect of cold exposure on 24 hr fasted mice. Unlike with 48 hr fasting, under 24 hr fasting conditions, *AceCS2*$^{-/-}$ mice maintained their core body temperatures at levels similar to *AceCS2*$^{+/+}$ mice, although both levels were equally reduced by 2°C–3°C compared to fed levels. Exposure of these mice to cold further decreased their core temperatures; however, after 5 hr cold exposure, there was no significant difference between *AceCS2*$^{-/-}$ and *AceCS2*$^{+/+}$ mice (Figure 3I, right panel). These data indicate that adaptive thermogenesis in response to low temperature was not impaired in *AceCS2*$^{-/-}$ mice and further suggest that the sympathetic nervous system is able to properly maintain core body temperature in *AceCS2*$^{-/-}$ mice.

We hypothesized that fasting *AceCS2*$^{-/-}$ mice would lead to decreased exercise tolerance, owing to impaired acetate oxidation and subsequent reduction of ATP production in skeletal muscle (Figure 3E). *AceCS2*$^{-/-}$ mice were exercised on a motorized treadmill apparatus using a run-to-exhaustion protocol. *AceCS2*$^{-/-}$ mice fasted for 48 hr exhibited a markedly reduced capacity to sustain running exercise, whereas the running capacity of *AceCS2*$^{+/+}$ mice did not change between the fed and fasted conditions (Figure 3J). This suggests that acetate is an important fuel required for exercise as well as for heat generation during fasting.

AceCS2$^{-/-}$ Mice Compensate for Metabolic Acidosis through Hyperventilation

Because the plasma acetate levels are very high in *AceCS2*$^{-/-}$ mice, we speculated that these mice could be acidotic, and, if not, they might be hyperventilating to blow off CO_2 to prevent acidemia. Accordingly, we measured the arterial blood gases, pH, and bicarbonate concentration. The values of arterial carbon dioxide partial pressure ($PaCO_2$) were significantly decreased in *AceCS2*$^{-/-}$ mice ($p < 0.05$, $n = 5–6$), indicating that *AceCS2*$^{-/-}$ mice were hyperventilating to blow off CO_2. There were no significant differences in the values of PaO_2, standardized bicarbonate concentration ($[HCO_3^-]$), and the pH (Table 1). These data indicate that *AceCS2*$^{-/-}$ mice were hyperventilating to compensate for a possible acidosis caused by acetate accumulation. This hyperventilation in *AceCS2*$^{-/-}$ mice might account for some of their increased energy expenditure compared to *AceCS2*$^{+/+}$ mice.

AceCS2$^{-/-}$ Mice Exhibit Hypothermia and Hypoglycemia under Low-Carbohydrate, High-Fat Diet

Similar to fasting conditions, we hypothesized that acetate utilization may be important under low-glucose or low-carbohydrate intake states. To examine this possibility, 4-week-old *AceCS2*$^{-/-}$ and *AceCS2*$^{+/+}$ mice were fed a low-carbohydrate, high-fat diet (LC/HF; 0.4% carbohydrate, 90.5% fat, and 9.1% protein from calories). At the time of weaning (4 weeks of age), *AceCS2*$^{-/-}$ mice weighed an average of 40% less than their littermates (Figures S1A–S1C), and plasma acetate levels were markedly elevated (Figure 4A). Plasma ketone bodies, NEFA, glucose, and insulin levels were comparable between *AceCS2*$^{+/+}$ and *AceCS2*$^{-/-}$ mice (Table S1).

On LC/HF diet, *AceCS2*$^{-/-}$ mice exhibited lower body temperatures (Figure 4B). This was most severe (30.1 ± 1.4°C) on day 2 of LC/HF diet feeding, whereas *AceCS2*$^{+/+}$ mice maintained their body temperatures at 37°C on this diet. In addition, *AceCS2*$^{-/-}$ mice lost weight, whereas the body weight of *AceCS2*$^{+/+}$ mice remained stable (Figure 4C). Furthermore, *AceCS2*$^{-/-}$ mice had sustained hypoglycemia (56 ± 5 mg/dl) over this period compared to *AceCS2*$^{+/+}$ mice that exhibited transiently decreased plasma glucose levels at weaning but soon recovered to normal levels (137 ± 7 mg/dl) (Figure 4D). This transient hypoglycemia in *AceCS2*$^{+/+}$ is most likely from the stress of forced weaning, which causes suppression of feeding on the day of weaning. Plasma NEFA and ketone body levels were highly elevated, but there were no significant differences between *AceCS2*$^{+/+}$ and *AceCS2*$^{-/-}$ mice except in ketone body levels on day 3 of the LC/HF diet (Figures 4E and 4F). The abundance of mRNAs for the enzymes involved in gluconeogenesis was not decreased in *AceCS2*$^{-/-}$ mice compared to *AceCS2*$^{+/+}$ mice (Figure S3A). Furthermore, injection of pyruvate to these mice rescued hypoglycemia (Figure S3B), indicating that the gluconeogenic pathway is intact.

Table 1. Blood Gas Analysis of *AceCS2*$^{+/+}$ and *AceCS2*$^{-/-}$ Mice

	+/+	−/−
pH	7.34 ± 0.03	7.34 ± 0.03
PaO_2 (mm Hg)	102.3 ± 2.7	108.8 ± 5.5
$PaCO_2$ (mm Hg)	37.3 ± 1.2	33.3 ± 0.9[a]
HCO_3^- (mM)	19.7 ± 0.8	17.6 ± 1.3
BE (mM)	−5.1 ± 1.2	−6.9 ± 1.9

Male mice (12 weeks old, n = 6 per genotype) were fed on a normal chow diet. Samples were obtained from the femoral artery of awake, freely moving mice. Data are mean ± SEM.
[a] $p < 0.05$ compared to *AceCS2*$^{+/+}$.

After 5 days of LC/HF diet feeding, *AceCS2*$^{-/-}$ mice began to die, and, by 21 days, 50% of the *AceCS2*$^{-/-}$ mice had died. By contrast, none of *AceCS2*$^{+/+}$ mice died (Figure 4G). However, following 21 days on the LC/HF diet, the surviving *AceCS2*$^{-/-}$ mice gradually recovered body temperature and plasma glucose levels. We observed no further excess mortality (data not shown).

Weight, body temperature, and plasma parameters (glucose, NEFA, and ketone bodies) did not differ significantly between the *AceCS2*$^{-/-}$ mice that died and those that survived during the 4 day period of LC/HF feeding after the weaning (Figures S4A–S4E). Therefore, the cause of death was not simply from malnutrition. We also examined the effect of a high-carbohydrate, high-fat (HC/HF) diet (58% fat, 15% protein, and 27% carbohydrate from calories). On this diet, both *AceCS2*$^{-/-}$ and *AceCS2*$^{+/+}$ mice survived with no deaths (data not shown). These data indicated that acetate oxidation mediated by AceCS2 is essential to maintain normal thermogenesis and fuel usage under low-glucose utilization states such as low-carbohydrate diets or fasting.

AceCS2$^{-/-}$ Mice Exhibit Low Body Weight Gain under Low Carbohydrate Intake

We continued to feed the surviving *AceCS2*$^{-/-}$ mice an LC/HF diet. *AceCS2*$^{+/+}$ mice fed on this diet gained weight efficiently; by contrast, *AceCS2*$^{-/-}$ mice exhibited reduced weight gain under this diet (Figure 5A). Food intake was unchanged between

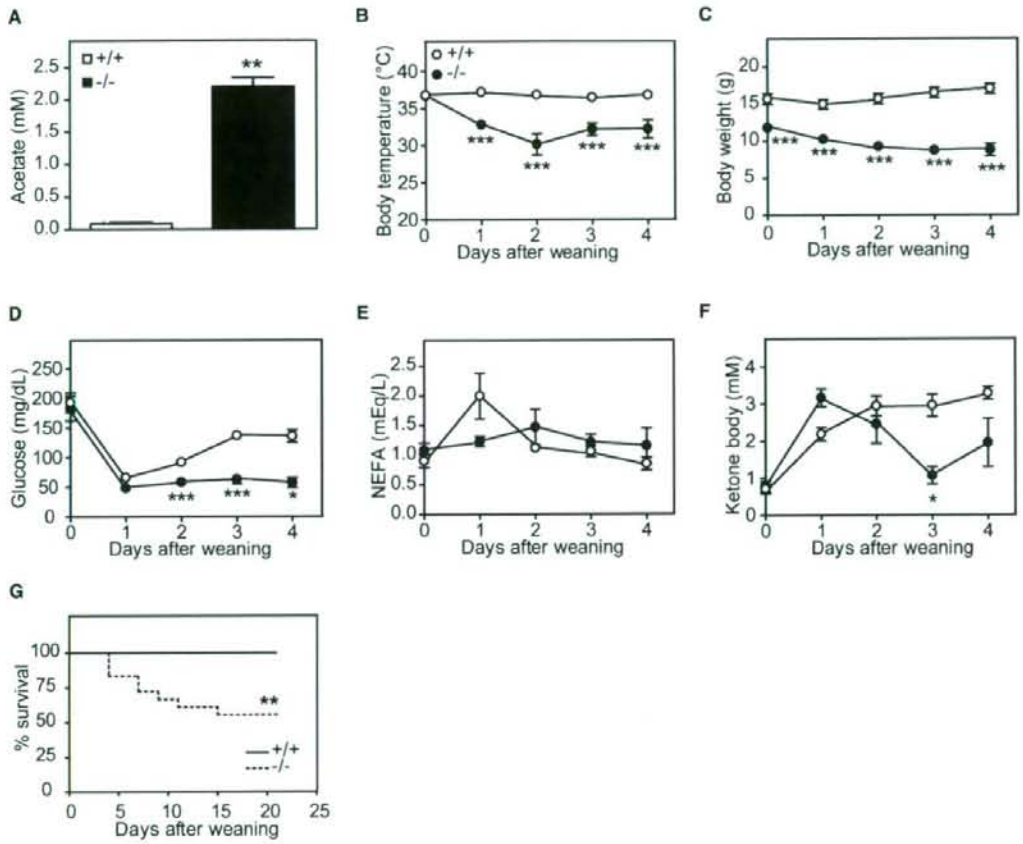

Figure 4. *AceCS2*-Deficient Mice Exhibit Hypothermia When Fed an LC/HF Diet

(A) Male mice (4 weeks old, five per genotype) were fed milk from their mother. Plasma acetate levels were measured.

(B–F) Male mice (4 weeks old) were fed an LC/HF diet. (B) Core rectal temperature, (C) body weight, (D) blood glucose, (E) plasma NEFA, and (F) plasma ketone body level were measured (*AceCS2*$^{+/+}$, n = 8; *AceCS2*$^{-/-}$, n = 7). *p < 0.05, **p < 0.01, and ***p < 0.001 compared to *AceCS2*$^{+/+}$.

(G) Kaplan-Meier analysis of survival in males fed an LC/HF diet at 4 weeks old (*AceCS2*$^{+/+}$, n = 22; *AceCS2*$^{-/-}$, n = 18). **p < 0.001 compared to *AceCS2*$^{+/+}$ by Log-rank test. Data are mean ± SEM.

AceCS2$^{+/+}$ and *AceCS2*$^{-/-}$ mice (Figure 5B). We excised various tissues from these mice and measured tissue weights. The photo shown in Figure 5C was taken for representative mice of each group. There were no marked differences in the weights of liver, kidney, BAT, and heart between *AceCS2*$^{+/+}$ and *AceCS2*$^{-/-}$ mice, but the fat pads of *AceCS2*$^{-/-}$ mice were significantly smaller than those of *AceCS2*$^{+/+}$ mice (Figure 5D). We measured metabolic parameters of these mice at 24 weeks of age (Table 2). Although the plasma glucose levels were unchanged, plasma insulin levels decreased significantly in *AceCS2*$^{-/-}$ mice as compared to *AceCS2*$^{+/+}$ mice. Plasma levels of leptin were 4-fold lower, but plasma acetate was 7-fold higher in *AceCS2*$^{-/-}$ mice (Table 2).

In order to investigate the mechanism underlying reduced weight gain in *AceCS2*$^{-/-}$ mice, food intake and energy expenditure were examined. *AceCS2*$^{-/-}$ mice exhibited consistently higher rates of oxygen consumption and, therefore, had higher metabolic rates than *AceCS2*$^{+/+}$ mice throughout day and night (Figure 5E). After adjusting for allometric scaling and gender, the effect of the *AceCS2*$^{-/-}$ allele was highly significant ($p < 0.01$, n = 7, multiple ANOVA) (Figure 5E, right panel). The respiratory quotient was 0.71 in both *AceCS2*$^{+/+}$ and *AceCS2*$^{-/-}$ mice (data not shown). These data suggested that the resistance to weight gain of *AceCS2*$^{-/-}$ mice may be, at least in part, due to increased energy expenditure. To examine the possibility that fatty acids synthesis is changed in *AceCS2*$^{-/-}$ mice, we measured malonyl-CoA levels and acetyl-CoA carboxylase (ACC) activity (Figure S5). Malonyl-CoA levels and ACC activity in skeletal muscle and BAT did not significantly differ between *AceCS2*$^{-/-}$ and *AceCS2*$^{+/+}$ mice (Figure S5). In liver, malonyl-CoA levels

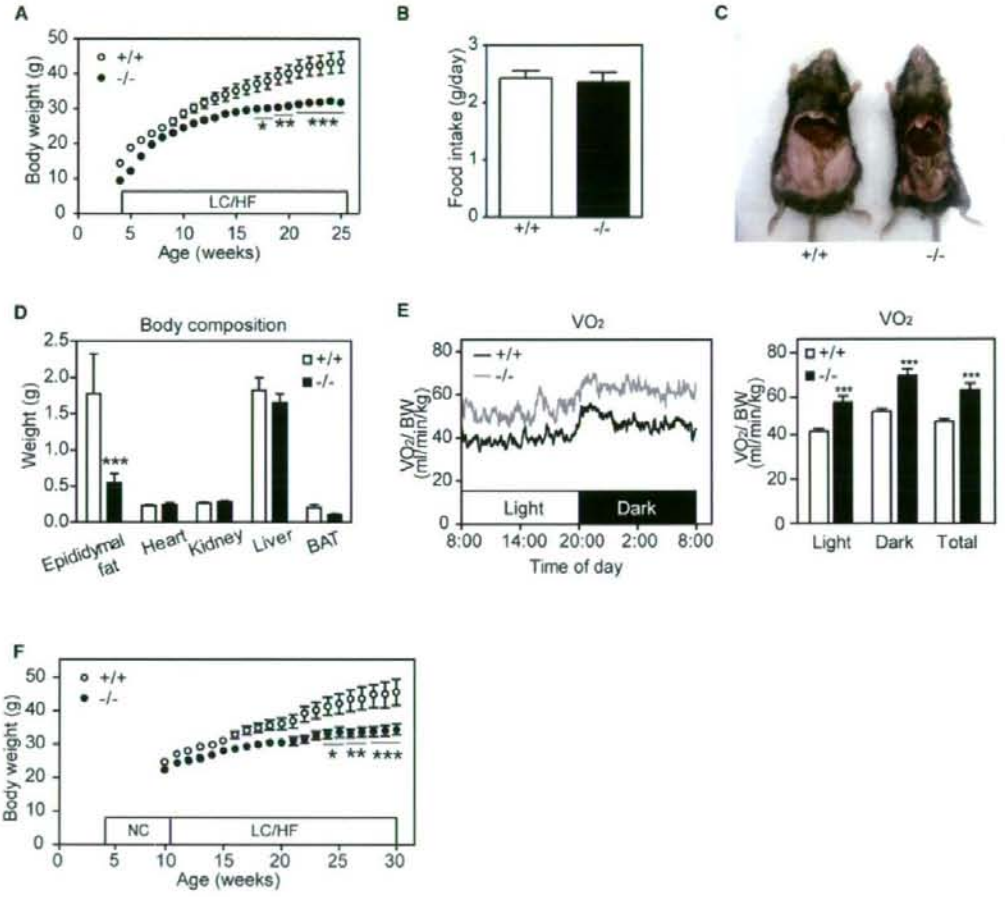

Figure 5. *AceCS2* Deficiency Attenuates Body Weight Gain in Mice Fed an LC/HF Diet

(A) Body weight change of male mice fed an LC/HF diet from 4 weeks old (*AceCS2*$^{+/+}$, n = 15; *AceCS2*$^{-/-}$, n = 12).

(B) Food intake of male mice fed an LC/HF diet at 25 weeks old (*AceCS2*$^{+/+}$, n = 15; *AceCS2*$^{-/-}$, n = 12).

(C) Representative picture of *AceCS2*$^{+/+}$ and *AceCS2*$^{-/-}$ male mice (26 weeks of age) fed an LC/HF diet.

(D) Various tissue weights for *AceCS2*$^{+/+}$ and *AceCS2*$^{-/-}$ male mice (26 weeks of age) fed an LC/HF diet (*AceCS* $^{+/+}$, n = 5; *AceCS2*$^{-/-}$, n = 5).

(E) Oxygen consumption (VO_2, left panel) and average of VO_2 (right panel) were determined in male mice (26 weeks old) fed an LC/HF diet by indirect calorimetry (*AceCS2*$^{+/+}$, n = 8; *AceCS2*$^{-/-}$, n = 7). Data are corrected for body weight. The original, uncorrected data are shown in Figure S6.

(F) Change of body weight. Male mice were weaned at 4 weeks and were fed on normal chow diet for 6 weeks (until 10 weeks of age) and switched to an LC/HF diet (*AceCS2*$^{+/+}$, n = 8; *AceCS2*$^{-/-}$, n = 8). *$p < 0.05$, **$p < 0.01$, and ***$p < 0.001$ compared to *AceCS2*$^{+/+}$. Data are mean ± SEM. NC, normal chow diet.

were reduced by 20% in *AceCS2*$^{-/-}$ (Figure S5), which could be the secondary effect of lower plasma insulin levels since AceCS2 is not expressed in liver. These data suggested that fatty acid synthesis and degradation are not impaired by the deficiency of *AceCS2*.

It is possible that the reduced weight gain of *AceCS2*$^{-/-}$ mice during LC/HF diet feeding simply resulted from a failure to thrive phenotype (reduced body weight gain, hypothermia, hypoglycemia, and low survival rate) induced by low-carbohydrate diet feeding immediately after weaning (Figure 4). Therefore, after weaning, we first fed the mice a normal chow diet for 6 weeks (until 10 weeks of age) and then switched them to an LC/HF diet. By contrast to feeding an LC/HF diet immediately after weaning, none of these *AceCS2*$^{-/-}$ mice died; however, they did exhibit reduced weight gain compared to *AceCS2*$^{+/+}$ mice following the switch to an LC/HF diet (Figure 5F). Reduced weight gain was observed only under a low-carbohydrate regimen. When mice were fed a high-fat, high-carbohydrate diet, *AceCS2*$^{-/-}$ mice were not protected against weight gain (data not shown). These results clearly indicate that adult

Table 2. Metabolic Parameters of *AceCS2*$^{-/-}$ and *AceCS2*$^{+/+}$ Mice Fed an LC/HF Diet

	+/+	−/−
Glucose (mg/dl)	233 ± 14	233 ± 22
Cholesterol (mg/dl)	110 ± 7	70 ± 11[b]
Triglycerides (mg/dl)	93 ± 6	92 ± 9
NEFA (μEql/l)	343 ± 17	332 ± 71
Ketone body (mM)	0.387 ± 0.064	0.705 ± 0.116[a]
Leptin (ng/ml)	2.80 ± 1.12	0.74 ± 1.03[b]
Insulin (ng/ml)	3.34 ± 1.3	1.54 ± 0.71[a]
Acetate (mM)	0.18 ± 0.06	0.97 ± 0.17[b]

Male mice (24 weeks old, seven to nine per genotype) were fed an LC/HF diet. Assays of blood samples were performed on isolated plasma.
[a] $p < 0.05$.
[b] $p < 0.01$ compared to *AceCS2*$^{+/+}$.

AceCS2$^{-/-}$ mice exhibit reduced adiposity under high-fat feeding, low-carbohydrate intake, or ketogenic conditions.

DISCUSSION

Under ketogenic conditions, free fatty acids are released into the circulation and taken up by thermogenic tissues such as BAT and skeletal muscle, where they serve as a fuel for thermogenesis (Picard et al., 2002; Spiegelman and Flier, 2001). Fatty acids are also taken up by liver for the generation of ketone bodies, and these ketone bodies are subsequently utilized in extrahepatic tissues. In addition, previous studies showed that an appreciable amount of acetate is generated in liver and this acetate can subsequently be utilized by extrahepatic tissues (Leighton et al., 1989; Murthy and Steiner, 1973; Seufert et al., 1974). Here, we demonstrate that acetate also serves as a fuel that has specific functions that do not overlap with those of fatty acids and ketone bodies in thermogenesis.

Our studies of mice with targeted deletion of *AceCS2* reveal that these animals can not maintain normal body temperature when starved or when fed an LC/HF diet. Under these conditions, *AceCS2*$^{-/-}$ mice display sustained hypoglycemia, strongly diminished capacity for exercise, and dramatically increased mortality as compared to their wild-type or heterozygous littermates. The mutant animals also exhibit strikingly reduced rates of whole-body acetate oxidation and correspondingly increased levels of acetate in plasma. Most importantly, ATP levels in the skeletal muscle of 48 hr fasted *AceCS2*$^{-/-}$ mice were profoundly reduced, showing the significant contribution of acetate and AceCS2 to the energy supply under ketogenic conditions. Therefore, under ketogenic conditions, the hypothermia and poor exercise tolerance observed in the *AceCS2*$^{-/-}$ mice is most likely from a lack of acetate utilization as a fuel source. Supporting this possibility, plasma acetate levels were significantly higher under fasting conditions than under fed conditions. This suggests that acetate turnover is significantly higher in the fasted state primarily due to AceCS2.

LC/HF diet has been generally recognized to have weight-reducing effects on obese animals (Kennedy et al., 2007). Although the body weight gain of mice fed an LC/HF diet is significantly lower than that of those fed high-fat and high-carbohydrate diets, our LC/HF diet has no weight-reducing or anti-weight-gaining effect. In the experiments done by Kennedy et al. (2007), 8-week-old mice fed a normal chow diet were switched to an LC/HF diet, and the weight of mice fed an LC/HF diet dropped until it stabilized at 85% of the initial weight. The discrepancy between these results may result from the difference in the composition of the different LC/HF diets. The LC/HF diet that Kennedy et al. used consists of 78.85% fat, 9.5% protein, and 0.76% carbohydrate, whereas our LC/HF diet (purchased from Harlan Teklad) contains 67.4% fat, 15.3% protein, and 0.6% carbohydrate (% by weight). In addition, the source of the fat is also different. The LC/HF diet in their study contains lard and butter, whereas our LC/HF diet contains vegetable shortening. Regardless of the differences in the exact diet, we show that AceCS2 is critical for normal body weight gain under an LC/HF diet.

Recent observations indirectly support a role for *AceCS2* as a determinant of growth and adiposity. From the mapping of a quantitative trait locus (QTL) region on mouse chromosome 2 that has a large effect on growth and adiposity, AceCS2 was reported as 1 of 18 candidate genes potentially controlling predisposition to growth and predisposition to obesity (Jerez-Timaure et al., 2005).

Although plasma acetate is very high in *AceCS2*$^{-/-}$ mice, we found that there was appropriate and sufficient respiratory compensation for any metabolic acidosis caused by acetate accumulation. *AceCS2*$^{-/-}$ mice exhibited hypocapnea to maintain a neutral arterial blood pH. Patients with chronic obstructive lung disease and cystic fibrosis commonly have low body weight, which is believed to be related to inadequate energy intake, nutrient malabsorption, and excessive energy expenditure (Bell et al., 1996). Basal metabolic rate is 10%–20% greater in these patients than in healthy subjects and may contribute to their energy imbalance. Furthermore, increased oxygen consumption caused by increased respiratory muscle activity has been reported in these patients, which largely explains the increased basal metabolic rate (Campbell et al., 1959; Cherniack, 1959; Donahoe et al., 1989; McGregor and Becklake, 1961). Because *AceCS2*$^{-/-}$ mice seem to be hyperventilating, this increased use of respiratory muscles might account for, at least in part, the higher oxygen consumption.

We previously identified AceCS2 as a target of KLF15 (Yamamoto et al., 2004). The fasting-induced transcription of AceCS2 is largely dependent on KLF15. Similarly to *AceCS2*$^{-/-}$ mice, KLF15-deficient mice also exhibit severe hypoglycemia after overnight fasting (Fisch et al., 2007). KLF15 plays an important role in gluconeogenesis by regulating amino acid degradation and key gluconeogenic enzymes such as phosphoenolpyruvate carboxykinase in the liver during fasting (Gray et al., 2007; Teshigawara et al., 2005). Our data indicate that KLF15 is crucial for survival during starvation through two mechanisms: (1) gluconeogenesis in liver and (2) acetate oxidation to generate ATP and heat in muscle and BAT through AceCS2 activity.

The sirtuins comprise a conserved family of proteins that are believed to mediate some of the health benefits of calorie restriction, which leads to extension of life span in nearly all organisms studied, including mammals. SIRT1 has been reported to function as an energy-sensing gene that senses NAD^+ levels and regulates the activity of critical transcriptional regulators of

metabolism in multiple tissues (Yang et al., 2007). Within the mitochondria, SIRT3 deacetylates a key lysine residue on AceCS2, leading to its enzymatic activation (Hallows et al., 2006; Schwer et al., 2006; Schwer and Verdin, 2008). As SIRT3 protein levels are specifically increased in calorie-restricted mammals, regulation of AceCS2 activity by SIRT3 could be a key metabolic factor responsible for homeostatic regulation during calorie restriction, leading to its positive effect on life span. Sirt3 was recently shown to be necessary for maintaining basal ATP levels with ATP levels in multiple organs of *Sirt3*$^{-/-}$ mice that are markedly reduced compared to wild-type levels (Ahn et al., 2008). This study, along with ours, suggests that activation of AceCS2 by Sirt3 is required to maintain basal ATP levels in mammals. Future studies of AceCS2- and AceCS2-deficient mice are warranted to investigate this potentially exciting link between longevity and mitochondrial energy metabolism.

In conclusion, our current findings demonstrate that acetate metabolism mediated by AceCS2 is crucial for survival and energy production under ketogenic conditions such as starvation or diabetes. These and future studies of acetate metabolism mediated by AceCS2 will have a significant impact on the understanding of the acetate metabolism for heat generation and energy metabolism.

EXPERIMENTAL PROCEDURES

Generation of AceCS2-Deficient Mice

We constructed a targeting plasmid by using genomic DNA fragments derived from Sv129 mice. A Lac Z and a neomycin cassette flanked by two loxP sites were introduced into the *AceCS2* locus of ES cells (derived from the Sv129 strain). Electroporation, selection, and screening were performed with standard gene-targeting techniques. Briefly, genomic DNA was isolated from neomycin-resistant ES cell clones, digested with KpnI, and subjected to hybridization with a probe to detect homologous recombination and the presence of the flox allele (Figure 1A).

Chimeric males were generated by using the morula aggregation technique and mated to C57BL/6J female mice. Homologous recombination was confirmed by Southern blotting (Figure 1B). Deletion of RNA transcripts and protein was confirmed by QRT-PCR and western blotting, respectively (Figures 1D and 1E). After achieving germline transmission, *AceCS2*$^{+/-}$ mice were crossed with C57BL/6J for six to nine generations.

Heterozygous mice were mated to obtain *AceCS2*$^{-/-}$ mice. Wild-type littermates were used as controls throughout the study. Genotyping of mice used in this study was performed by PCR of tail DNA as shown in Figure 1C; the mutant allele was detected by using a pair of oligonucleotides (5′-GGCGCACAACAAAACCTAGT-3′ and 5′-GACAGTATCGGCCTCAGGAA-3′) that amplify a 512 bp PCR product between the *AceCS2* and sequence 3′ to *Lac Z/neo* cassette. The wild-type allele was detected by PCR with a pair of oligonucleotides (5′-GGCGCACAACAAAACCTAGT-3′ and 5′-GGGGTTCGTGCCTGGTTG-3′) that amplify a 355 bp PCR product spanning exon 1.

Quantitative Real-Time PCR

Quantitative real-time PCR (QRT-PCR) was performed as previously described (Tanaka et al., 2003). All primer sequences used in this paper are available upon request.

Antibody

To produce rabbit polyclonal anti-murine AceCS2 (IgGA001), a 12-residue peptide corresponding to the C terminus of murine AceCS2 (CQKYEEQ RAATN) was synthesized (Sigma Genesis, Japan), coupled to keyhole limpet hemocyanin, and injected into New Zealand White rabbits. IgG fractions were prepared by affinity chromatography on protein A-Sepharose (GE Healthcare Bioscience). For immunoblot analysis, an aliquot of whole-cell lysates from heart (20 μg) was subjected to SDS-PAGE on 10% gels followed by analysis with a 1:1000 dilution of anti-AceCS2 (Fujino et al., 2001).

Animal Experiments

All procedures were performed in accordance with Japanese Physiological Society guidelines for animal care. Mice were group housed in cages with a 12 hr light/12 hr dark cycle and fed a standard rodent chow diet (CE-2; CLEA Japan, Osaka). To induce a ketogenic condition, we compared an LC/HF diet (Table S3; Rho et al., 1999) (TD96355; Harlan Teklad Premier Laboratory Diets) consisting of 90.5% fat, 9.1% protein, and 0.4% carbohydrate (0% sucrose from calories) to a high-carbohydrate, high-fat diet consisting of 58.0% fat, 15.0% protein, and 27.01% carbohydrate from calories (Tanaka et al., 2003). All mice had free access to water. Food consumption was monitored daily, and body weight was recorded every week, unless otherwise stated.

Core body temperature was monitored using a rectal thermometer at 10 a.m. For the exercise performance, the mice were trained on the treadmill (MK-680AT/02M, Muromachikikai, Tokyo) prior to the exercise performance test (a 10 min run at 10 m/min at a 5° incline once per day for 4 days). Exhaustion was defined as the point at which mice were unable to continue running.

Food Intake, Locomotor Activity, and Metabolic Rate Measurement

Male mice (26 weeks old) were housed under controlled lighting (12 hr light-dark cycle) and temperature (23°C) conditions. Food (standard chow pellets or an LC/HF diet) and water were available ad libitum. Mice were then housed singly under the same conditions as above for an acclimation period of at least 7 days. Body weights and food intake were monitored daily for the duration of the study. Energy expenditure was measured by indirect calorimetry as described previously (MK-5000RQ; Muromachi, Tokyo) (Takayasu et al., 2006). Mice were placed in the calorimeter chambers and acclimated for 1 day. Locomotor activity was measured by using an infrared (IR) passive sensor system as described previously (Supermex, Muromachi Kikai, Japan) (Takayasu et al., 2006). The experiment was started at 8 a.m. (light period).

Acetate Oxidation

Acetate ([1-^{14}C]acetate, CFA13, GE Healthcare UK Limited) oxidation was measured in vivo as described (Wolfgang et al., 2006). The in vivo rate of ^{14}C-acetate oxidation (2 μCi [1 Ci = 37 GBq] of [1-^{14}C]acetate injected intraperitoneally) to $^{14}CO_2$ was determined after treatment of mice. Mice were acclimated in metabolic chambers fitted with 2-aminoethanol traps to recover expired $^{14}CO_2$. The oxidation of [1-^{14}C]acetate to form $^{14}CO_2$ was measured at 20 min intervals over the next 1 hr. At the end of experiment, plasma was collected, and plasma [1-^{14}C]acetate was measured.

Acetate Measurement

Plasma acetate levels were measured as described by (Hillman et al. 1978) with slight modifications. Briefly, plasma was mixed with 1 mM isovaleric acid as the internal standard. The sample was acidified with one-fifth the volume of 10% sulfosalicylic acid and then extracted three times with 10 volumes of diethylether. The ether extract was immediately back extracted into 0.2 M NaOH. The ether was removed under a stream of dry nitrogen. Before injection, the sample was reacidified with one-fifth the volume of 10% phosphoric acid. The acetate concentration of the sample was analyzed by gas chromatograph (GC-2014, Shimadzu, Japan) equipped with a flame ionization detector and a capillary column (ULBON HR-20 M, 0.25 mm i.d. × 25 m × 0.25 μm). The column was operated at 140°C. The injection port and the flame ionization detector were maintained at 300°C. The chromatograph was standardized with a mixture of C2-C7 short-chain fatty acids.

Plasma Parameters

Mice were sacrificed by CO_2 asphyxiation following a 4 hr fast during the light cycle (food removed 9:00 a.m., sacrificed at 1:00 p.m.). Blood was drawn by cardiac puncture, and the plasma was separated immediately by centrifugation and stored at −80°C until use. Plasma glucose, NEFA, triglycerides, total cholesterol, and total ketone body levels were determined by Glucose C2-test (Wako Pure Chemical, Japan), NEFA C-test (Wako Pure Chemical, Japan), Triglyceride E-test (Wako Pure Chemical, Japan), Cholesterol E-test (Wako Pure Chemical, Japan), and Autokit Total Ketone Bodies (Wako Pure

Chemical, Japan), respectively. Plasma insulin and leptin levels were determined by ELISA with an insulin immunoassay kit (Shibayagi, Japan) and a mouse leptin immunoassay (R & D systems) according to the manufacturer's instructions.

Assay Procedure for Acetyl-CoA, Adenine Nucleotides, NAD$^+$, and NADH Contents

Acetyl-CoA and adenine nucleotide contents in skeletal muscle or BAT of 12-week-old male mice were measured essentially as described previously (Miura et al., 2006; Scott et al., 1992; Takamura et al., 1985). NAD$^+$ and NADH nucleotide concentrations were directly measured by NAD$^+$/NADH Assay kit (Biochain Institute, Inc.) according to the manufacturer's instructions. The detail methods are described in the Supplemental Experimental Procedures.

Blood Gas Analysis

Blood gas analysis was performed as previously described (Kuwaki et al., 1996). A catheter was implanted into the right femoral artery under isoflurane (2%–3%) anesthesia. Up to 70 μl of arterial blood was drawn from the indwelling catheter after a recovery period of more than 2 hr and when the animal was quietly awake. Blood gases were determined by a blood gas analyzer (ABL500, Radiometer, Copenhagen).

Statistical Analyses

All values are expressed as mean ± standard error of the mean unless otherwise specified. Significant differences between mean values were evaluated using two-tailed, unpaired Student's t test (when two groups were analyzed) or one-way ANOVA followed by Student Newman-Keuls test (for three or more groups).

SUPPLEMENTAL DATA

Supplemental Data include Supplemental Experimental Procedures, six figures, and three tables and can be found with this article online at: http://www.cell.com/cell-metabolism/supplemental/S1550-4131(08)00393-8.

ACKNOWLEDGMENTS

We thank Dr. Rob Rawson for critical reading of the manuscript; Drs. Peter Edwards and Mitsuhiro Watanabe for helpful discussions; and Kaori Ikeda, Junko Kuno, Satomi Takahashi, Yuko Kai, and Mika Nomiyama for technical assistance. This work was supported through ERATO JST, NIBIO by the NFAT project of the NEDO and by the Special Coordination Fund for Science and Technology from the Ministry of Education, Culture, Sports, Science, and Technology. This work was also supported, in part, by Astellas Foundation for Research on Metabolic Disorders, the Uehara Memorial Foundation, and the Ono Medical Foundation. M.Y. is an Investigator of the Howard Hughes Medical Institute. J.S. is an Investigator of Translational Systems Biology and Medicine Initiative (TSBMI).

Received: June 6, 2008
Revised: October 15, 2008
Accepted: December 12, 2008
Published: February 3, 2009

REFERENCES

Ahn, B.H., Kim, H.S., Song, S., Lee, I.H., Liu, J., Vassilopoulos, A., Deng, C.X., and Finkel, T. (2008). A role for the mitochondrial deacetylase Sirt3 in regulating energy homeostasis. Proc. Natl. Acad. Sci. USA *105*, 14447–14452.

Bell, S.C., Saunders, M.J., Elborn, J.S., and Shale, D.J. (1996). Resting energy expenditure and oxygen cost of breathing in patients with cystic fibrosis. Thorax *51*, 126–131.

Campbell, E.J., Westlake, E.K., and Cherniack, R.M. (1959). The oxygen consumption and efficiency of the respiratory muscles of young male subjects. Clin. Sci. (Lond.) *18*, 55–64.

Cherniack, R.M. (1959). The oxygen consumption and efficiency of the respiratory muscles in health and emphysema. J. Clin. Invest. *38*, 494–499.

Donahoe, M., Rogers, R.M., Wilson, D.O., and Pennock, B.E. (1989). Oxygen consumption of the respiratory muscles in normal and in malnourished patients with chronic obstructive pulmonary disease. Am. Rev. Respir. Dis. *140*, 385–391.

Fisch, S., Gray, S., Heymans, S., Haldar, S.M., Wang, B., Pfister, O., Cui, L., Kumar, A., Lin, Z., Sen-Banerjee, S., et al. (2007). Kruppel-like factor 15 is a regulator of cardiomyocyte hypertrophy. Proc. Natl. Acad. Sci. USA *104*, 7074–7079.

Fujino, T., Kondo, J., Ishikawa, M., Morikawa, K., and Yamamoto, T.T. (2001). Acetyl-CoA synthetase 2, a mitochondrial matrix enzyme involved in the oxidation of acetate. J. Biol. Chem. *276*, 11420–11426.

Fukao, T., Lopaschuk, G.D., and Mitchell, G.A. (2004). Pathways and control of ketone body metabolism: On the fringe of lipid biochemistry. Prostaglandins Leukot. Essent. Fatty Acids *70*, 243–251.

Gray, S., Wang, B., Orihuela, Y., Hong, E.G., Fisch, S., Haldar, S., Cline, G.W., Kim, J.K., Peroni, O.D., Kahn, B.B., et al. (2007). Regulation of gluconeogenesis by Kruppel-like factor 15. Cell Metab. *5*, 305–312.

Hallows, W.C., Lee, S., and Denu, J.M. (2006). Sirtuins deacetylate and activate mammalian acetyl-CoA synthetases. Proc. Natl. Acad. Sci. USA *103*, 10230–10235.

Hillman, R.E. (1978). Simple, rapid method for determination of propionic acid and other short-chain fatty acids in serum. Clin. Chem. *24*, 800–803.

Ikeda, Y., Yamamoto, J., Okamura, M., Fujino, T., Takahashi, S., Takeuchi, K., Osborne, T.F., Yamamoto, T.T., Ito, S., and Sakai, J. (2001). Transcriptional regulation of the murine acetyl-CoA synthetase 1 gene through multiple clustered binding sites for sterol regulatory element-binding proteins and a single neighboring site for Sp1. J. Biol. Chem. *276*, 34259–34269.

Jerez-Timaure, N.C., Eisen, E.J., and Pomp, D. (2005). Fine mapping of a QTL region with large effects on growth and fatness on mouse chromosome 2. Physiol. Genomics *21*, 411–422.

Kennedy, A.R., Pissios, P., Otu, H., Xue, B., Asakura, K., Furukawa, N., Marino, F.E., Liu, F.F., Kahn, B.B., Libermann, T.A., et al. (2007). A high-fat, ketogenic diet induces a unique metabolic state in mice. Am. J. Physiol. Endocrinol. Metab. *292*, E1724–E1739.

Kuwaki, T., Cao, W.H., Kurihara, Y., Kurihara, H., Ling, G.Y., Onodera, M., Ju, K.H., Yazaki, Y., and Kumada, M. (1996). Impaired ventilatory responses to hypoxia and hypercapnia in mutant mice deficient in endothelin-1. Am. J. Physiol. *270*, R1279–R1286.

Leighton, F., Bergseth, S., Rortveit, T., Christiansen, E.N., and Bremer, J. (1989). Free acetate production by rat hepatocytes during peroxisomal fatty acid and dicarboxylic acid oxidation. J. Biol. Chem. *264*, 10347–10350.

Lowell, B.B., and Spiegelman, B.M. (2000). Towards a molecular understanding of adaptive thermogenesis. Nature *404*, 652–660.

Luong, A., Hannah, V.C., Brown, M.S., and Goldstein, J.L. (2000). Molecular characterization of human acetyl-CoA synthetase, an enzyme regulated by sterol regulatory element-binding proteins. J. Biol. Chem. *275*, 26458–26466.

Matthias, A., Ohlson, K.B., Fredriksson, J.M., Jacobsson, A., Nedergaard, J., and Cannon, B. (2000). Thermogenic responses in brown fat cells are fully UCP1-dependent. UCP2 or UCP3 do not substitute for UCP1 in adrenergically or fatty scid-induced thermogenesis. J. Biol. Chem. *275*, 25073–25081.

McGregor, M., and Becklake, M.R. (1961). The relationship of oxygen cost of breathing to respiratory mechanical work and respiratory force. J. Clin. Invest. *40*, 971–980.

Miura, S., Tomitsuka, E., Kamei, Y., Yamazaki, T., Kai, Y., Tamura, M., Kita, K., Nishino, I., and Ezaki, O. (2006). Overexpression of peroxisome proliferator-activated receptor gamma co-activator-1alpha leads to muscle atrophy with depletion of ATP. Am. J. Pathol. *169*, 1129–1139.

Murthy, V.K., and Steiner, G. (1973). Hepatic acetate levels in relation to altered lipid metabolism. Metabolism *22*, 81–84.

Picard, F., Gehin, M., Annicotte, J., Rocchi, S., Champy, M.F., O'Malley, B.W., Chambon, P., and Auwerx, J. (2002). SRC-1 and TIF2 control energy balance between white and brown adipose tissues. Cell *111*, 931–941.

Rho, J.M., Kim, D.W., Robbins, C.A., Anderson, G.D., and Schwartzkroin, P.A. (1999). Age-dependent differences in flurothyl seizure sensitivity in mice treated with a ketogenic diet. Epilepsy Res. *37*, 233–240.

Schwer, B., Bunkenborg, J., Verdin, R.O., Andersen, J.S., and Verdin, E. (2006). Reversible lysine acetylation controls the activity of the mitochondrial enzyme acetyl-CoA synthetase 2. Proc. Natl. Acad. Sci. USA *103*, 10224–10229.

Schwer, B., and Verdin, E. (2008). Conserved metabolic regulatory functions of sirtuins. Cell Metab. *7*, 104–112.

Scott, M.D., Baudendistel, L.J., and Dahms, T.E. (1992). Rapid separation of creatine, phosphocreatine and adenosine metabolites by ion-pair reversed-phase high-performance liquid chromatography in plasma and cardiac tissue. J. Chromatogr. *576*, 149–154.

Seufert, C.D., Graf, M., Janson, G., Kuhn, A., and Soling, H.D. (1974). Formation of free acetate by isolated perfused livers from normal, starved and diabetic rats. Biochem. Biophys. Res. Commun. *57*, 901–909.

Spiegelman, B.M., and Flier, J.S. (2001). Obesity and the regulation of energy balance. Cell *104*, 531–543.

Takamura, Y., Kitayama, Y., Arakawa, A., Yamanaka, S., Tosaki, M., and Ogawa, Y. (1985). Malonyl-CoA: Acetyl-CoA cycling. A new micromethod for determination of acyl-CoAs with malonate decarboxylase. Biochim. Biophys. Acta *834*, 1–7.

Takayasu, S., Sakurai, T., Iwasaki, S., Teranishi, H., Yamanaka, A., Williams, S.C., Iguchi, H., Kawasawa, Y.I., Ikeda, Y., Sakakibara, I., et al. (2006). A neuropeptide ligand of the G protein-coupled receptor GPR103 regulates feeding, behavioral arousal, and blood pressure in mice. Proc. Natl. Acad. Sci. USA *103*, 7438–7443.

Tanaka, T., Yamamoto, J., Iwasaki, S., Asaba, H., Hamura, H., Ikeda, Y., Watanabe, M., Magoori, K., Ioka, R.X., Tachibana, K., et al. (2003). Activation of peroxisome proliferator-activated receptor delta induces fatty acid beta-oxidation in skeletal muscle and attenuates metabolic syndrome. Proc. Natl. Acad. Sci. USA *100*, 15924–15929.

Teshigawara, K., Ogawa, W., Mori, T., Matsuki, Y., Watanabe, E., Hiramatsu, R., Inoue, H., Miyake, K., Sakaue, H., and Kasuga, M. (2005). Role of Kruppel-like factor 15 in PEPCK gene expression in the liver. Biochem. Biophys. Res. Commun. *327*, 920–926.

Wolfgang, M.J., Kurama, T., Dai, Y., Suwa, A., Asaumi, M., Matsumoto, S., Cha, S.H., Shimokawa, T., and Lane, M.D. (2006). The brain-specific carnitine palmitoyltransferase-1c regulates energy homeostasis. Proc. Natl. Acad. Sci. USA *103*, 7282–7287.

Yamamoto, J., Ikeda, Y., Iguchi, H., Fujino, T., Tanaka, T., Asaba, H., Iwasaki, S., Ioka, R.X., Kaneko, I.W., Magoori, K., et al. (2004). A Kruppel-like factor KLF15 contributes fasting-induced transcriptional activation of mitochondrial acetyl-CoA synthetase gene AceCS2. J. Biol. Chem. *279*, 16954–16962.

Yamashita, H., Kaneyuki, T., and Tagawa, K. (2001). Production of acetate in the liver and its utilization in peripheral tissues. Biochim. Biophys. Acta *1532*, 79–87.

Yang, H., Yang, T., Baur, J.A., Perez, E., Matsui, T., Carmona, J.J., Lamming, D.W., Souza-Pinto, N.C., Bohr, V.A., Rosenzweig, A., et al. (2007). Nutrient-sensitive mitochondrial NAD+ levels dictate cell survival. Cell *130*, 1095–1107.

JACS
JOURNAL OF THE AMERICAN CHEMICAL SOCIETY

Communication

Lanthanide-Based Protease Activity Sensors for Time-Resolved Fluorescence Measurements

Shin Mizukami, Kazuhiro Tonai, Masahiro Kaneko, and Kazuya Kikuchi

J. Am. Chem. Soc., **2008**, 130 (44), 14376-14377• DOI: 10.1021/ja800322b • Publication Date (Web): 08 October 2008

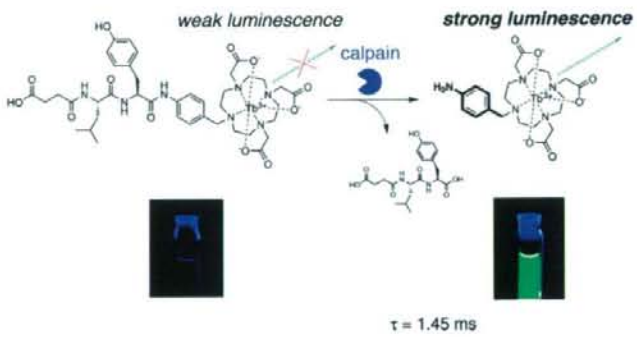

More About This Article

Additional resources and features associated with this article are available within the HTML version:

- Supporting Information
- Access to high resolution figures
- Links to articles and content related to this article
- Copyright permission to reproduce figures and/or text from this article

View the Full Text HTML

J|A|C|S
COMMUNICATIONS

Published on Web 10/08/2008

Lanthanide-Based Protease Activity Sensors for Time-Resolved Fluorescence Measurements

Shin Mizukami, Kazuhiro Tonai, Masahiro Kaneko, and Kazuya Kikuchi*

Division of Advanced Science and Biotechnology, Graduate School of Engineering, Osaka University, 2-1 Yamadaoka, Suita, Osaka 565-0871, Japan

Received January 15, 2008; E-mail: kkikuchi@mls.eng.osaka-u.ac.jp

Time-resolved fluorescence measurements with long-lifetime luminescent lanthanide complexes[1] have attracted great attention from scientists. This is because the time-resolved luminescence signals are highly sensitive and are scarcely affected by other fluorescent compounds that coexist in the sample, which often interfere with steady-state fluorescence measurements. This method is quite useful, especially in high-throughput drug screening.[2] Protease inhibitors can be important drug targets for diverse diseases, including cancer, AIDS, inflammatory disorders, and so on. Therefore, lanthanide-based luminescent sensors that detect protease activities assume great significance.

Karvinen et al. reported a protease assay based on time-resolved fluorescence resonance energy transfer (TR-FRET).[3] However, the synthesis of TR-FRET probes is generally laborious because it involves the attachment of both the luminescent lanthanide complex and the appropriate quencher on the substrate peptides. Additionally, when the probe concentration is high, this system is associated with the risk of diffusion-enhanced intermolecular FRET.[4] Although another simpler assay based on quenching by photoinduced electron transfer is known, the luminescent substrate becomes nonluminescent after enzyme reaction in this case.[5] In principle, such quenching-type fluorescent probes are inferior to fluorogenic probes, which fluoresce after enzyme reaction, because fluorescence is generally quenched by several factors such as collisional quenching, energy transfer, electron transfer, and so on. Besides TR-FRET probes, there exist no other fluorogenic protease probes based on lanthanide luminescence. Therefore, fluorogenic probes such as substrate peptides attached with the short-lifetime fluorophore MCA (4-methylcoumarinyl-7-amide) are widely used in protease assays, despite the above-described limitations.[6] We here report simple-structure luminogenic lanthanide probes that detect protease activities.

The long-lifetime luminescence of lanthanide ions is due to the forbidden f−f transitions of metal electrons. Generally, energy transfer from an adjacent chromophore to a lanthanide ion is utilized for the efficient excitation of lanthanide ions. The structures of the antenna chromophores regulate the lanthanide luminescence intensity.[7] Thus, the antenna groups can be strategic targets for designing luminogenic lanthanide probes. By modifying the antenna structures, several kinds of lanthanide-based probes have been developed so far, for instance, for detecting pH,[8] metal ions,[9] and other molecules.[10] To develop luminogenic lanthanide probes for detecting protease activities, the candidate antenna groups should fulfill two requirements: (1) antenna groups with an amino group should yield strong lanthanide luminescence and (2) the lanthanide luminescence should be very weak when the amino group is protected with an acyl group. We thoroughly investigated the known antenna groups for the above requirements. We found that very few antenna groups that have an amino group could emit lanthanide luminescence in aqueous solution.[11] We considered this is because

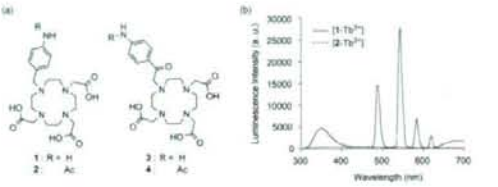

Figure 1. (a) Structures of synthesized compounds; (b) emission spectra of [**1**-Tb^{3+}] and [**2**-Tb^{3+}]; λ_{ex} = 250 nm.

Scheme 1. Structures and Schematic Representation of the Probes for Detecting Protease Activity

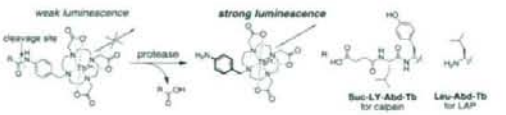

amino groups generally function as quenching groups for lanthanide luminescence.[5,12,13] Generally, amino substituents cause the red shift of the absorption spectra, and long-wavelength dyes are not adequate for the efficient excitation of Tb^{3+} or Eu^{3+}.[12] Thus, we hypothesized that only simple aromatic compounds with an amino group can act as efficient antenna groups for luminescent lanthanide ions such as Tb^{3+} and Eu^{3+}. Since tyrosine is known to sensitize Tb^{3+} and Eu^{3+},[14] we expected that even aniline derivatives could serve as good antenna groups.

For confirming the hypothesis, we designed and synthesized antenna-chelator conjugates **1** and **3**, which have simple aniline derivative groups as the antennas, and the corresponding acetylated compounds **2** and **4** (Figure 1a). We chose DO3A (1,4,7-tricarboxymethyl-1,4,7,10-tetraazacyclododecane) as the chelator for its strong binding ability to trivalent lanthanide ions.[15] The complex [**1**-Tb^{3+}] showed the characteristic emission spectrum of lanthanide complexes besides the antenna fluorescence at 350 nm (Figure 1b). Meanwhile, [**2**-Tb^{3+}]—the Tb^{3+} complex of the acetylated compound **2**—did not show lanthanide luminescence. On the other hand, although [**3**-Tb^{3+}] did not show lanthanide luminescence, [**4**-Tb^{3+}] showed strong lanthanide luminescence (see Supporting Information). Since the two acetylated compounds **2** and **4** are the model compounds of peptide conjugates, the above results indicated that the 4-aminobenzyl group can be a suitable antenna for luminogenic lanthanide probes detecting protease activities and that 4-aminobenzoylmethyl group can be an antenna for quenching-type protease probes. In addition, none of the Eu^{3+} complexes of compounds **1**−**4** showed lanthanide luminescence (data not shown).

Next, we designed Suc-LY-Abd-Tb to detect calpain activity, as shown in Scheme 1. Calpains are a family of intracellular cysteine proteases that are involved in many cellular processes.[16] Calpains

10.1021/ja800322b CCC: $40.75

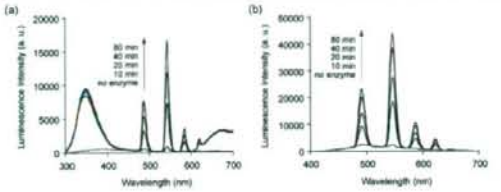

Figure 2. (a) Steady-state and (b) time-resolved (delay time, 10 μs; gate time, 3.0 ms) emission spectral change of Suc-LY-Abd-Tb with calpain I. λ_{ex} = 250 nm.

Table 1. Photophysical Properties of the Synthesized Compounds

	λ_{abs}/nm	ϵ/M^{-1} cm^{-1}	Φ	τ/ms
[**1**-Tb^{3+}]	240	12 000	0.051	1.47
[**2**-Tb^{3+}]	284	3 500	<0.001	1.49
Suc-LY-Abd-Tb	254	11 000	<0.001	1.46
Suc-LY-Abd-Tb + calpain I[a]	263	13 000	0.012	1.45

[a] It was confirmed by reversed-phase HPLC that enzyme reaction was completed.

are also related to several diseases such as muscular dystrophy, Alzheimer's disease, Parkinson's disease, and so on.[17] Thus, highly sensitive detection methods for calpain activities are crucial for developing drugs for such diseases.[18] The peptide sequence Suc-LY is known to be recognized efficiently by both calpains I and II.[17] The peptide-ligand conjugate Suc-LY-Abd was synthesized by a liquid-phase method, and the ligand was then complexed with Tb^{3+}. As we expected, the emission spectrum of Suc-LY-Abd-Tb was scarcely luminescent, similar to that of [**2**-Tb^{3+}]. Then, the addition of calpain I to the Suc-LY-Abd-Tb solution increased the emission intensity in a time-dependent manner (Figure 2a). The steady-state spectra in Figure 2a also include fluorescence around 350 nm derived from the antenna and the protein. In such cases, time-resolved measurement is very effective. The luminescence lifetimes of the synthesized compounds were approximately 1.5 ms (Table 1), much longer than those of general organic fluorescent compounds. Thus, the short-lifetime components in the emission spectra were completely excluded by performing measurements after a delay of 10 μs (Figure 2b).

We investigated the practical usefulness of Suc-LY-Abd-Tb. When fluorescent molecules are present in samples, they are very likely to significantly affect the results of fluorescence assays. For example, fluorescent drug candidates would give rise to false results for enzyme screening assays. We performed calpain assays with Suc-LY-Abd-Tb and the commercial probe Suc-LY-MCA in the presence of fluorescent compounds such as umbelliferone. The fluorescence intensity of Suc-LY-MCA was considerably increased in the presence of such compounds as compared to that in their absence. The time-resolved fluorescence intensity of Suc-LY-Abd-Tb was barely affected under the same conditions (see Supporting Information). This result indicates the superiority of our lanthanide-based probes over conventional fluorescent probes in practical applications.

Finally, to demonstrate the generality of our sensing system, we synthesized another lanthanide-based probe, Leu-Abd-Tb, for leucine aminopeptidase (LAP); this enzyme hydrolyzes the peptide bond of N-terminal hydrophobic amino acids such as leucine (Scheme 1). Leu-Abd-Tb showed an increase in the time-resolved luminescence when incubated with LAP (see Supporting Information), similar to the case of Suc-LY-Abd.

In conclusion, we developed novel luminogenic lanthanide probes for detecting protease activities. The probe design principle could be widely applicable to time-resolved assays for any proteases. These lanthanide-based probes could accelerate drug-screening processes and also contribute to the clarification of biological systems. Furthermore, achievement of longer wavelength excitation could enable a microscopic time-resolved fluorescence imaging of protease activities in living cells.[13]

Acknowledgment. We thank MEXT of Japan and JST for the financial supports. We thank Dr. Tomoyoshi Suenobu for the technical support for time-resolved fluorescence measurement.

Supporting Information Available: Detailed synthetic procedures; supplementary spectra; physical properties; photostability experiment; enzyme reaction experiment. This material is available free of charge via the Internet at http://pubs.acs.org.

References

(1) (a) Bünzli, J.-C. G.; Piguet, C. *Chem. Soc. Rev.* **2005**, *34*, 1048–1077. (b) Yuan, J.; Wang, G. *Trends Anal. Chem.* **2006**, *25*, 490–500.
(2) Kumar, R. A.; Clark, D. S. *Curr. Opin. Chem. Biol.* **2006**, *10*, 162–168.
(3) (a) Karvinen, J.; Laitala, V.; Mäkinen, M.-L.; Mulari, O.; Tamminen, J.; Hermonen, J.; Hurskainen, P.; Hammilä, I. *Anal. Chem.* **2004**, *76*, 1429–1436. (b) Karvinen, J.; Elomaa, A.; Mäkinen, M. -L.; Hakala, H.; Mukkala, V. -M.; Peuralahti, J.; Hurskainen, P.; Hovinen, J.; Hemmilä, I. *Anal. Biochem.* **2004**, *325*, 317–325.
(4) Stryer, L.; Thomas, D. D.; Meares, C. F. *Annu. Rev. Biophys. Bioeng.* **1982**, *11*, 203–222.
(5) Terai, T.; Kikuchi, K.; Iwasawa, S.; Kawabe, T.; Hirata, Y.; Urano, Y.; Nagano, T. *J. Am. Chem. Soc.* **2006**, *128*, 6938–6946.
(6) (a) Rano, T. A.; Timkey, T.; Peterson, E. P.; Rotonda, J.; Nicholson, D. W.; Becker, J. W.; Chapman, K. T.; Thornberry, N. A. *Chem. Biol.* **1997**, *4*, 149–155. (b) Harris, J. L.; Backes, B. J.; Leonetti, F.; Mahrus, S.; Ellman, J. A.; Craik, C. S. *Proc. Natl. Acad. Sci. U.S.A.* **2000**, *97*, 7754–7759. (c) Salisbury, C. M.; Maly, D. J.; Ellman, J. A. *J. Am. Chem. Soc.* **2002**, *124*, 14868–14870.
(7) Latva, M.; Takalo, H.; Mukkala, V. -M.; Matachescu, C.; Rodriguez-Ubis, J. C.; Kankare, J. *J. Lumin.* **1997**, *75*, 149–169.
(8) (a) de Silva, A. P; Gunaratne, H. Q. N.; Rice, T. E. *Angew. Chem., Int. Ed. Engl.* **1996**, *35*, 2116–2118. (b) Parker, D.; Senanayake, P. K.; Williams, J. A. G. *J. Chem. Soc., Perkin Trans. 2* **1998**, 2129–2139. (c) Gunnlaugsson, T.; Mac Dónaill, D. A.; Parker, D. *J. Am. Chem. Soc.* **2001**, *123*, 12866–12876. (d) Gunnlaugsson, T.; Leonard, J. P.; Sénéchal, K.; Harte, A. J. *J. Am. Chem. Soc.* **2004**, *126*, 12470–12476.
(9) (a) de Silva, A. P; Gunaratne, H. Q. N.; Rice, T. E.; Stewart, S. *Chem. Commun.* **1997**, 1891–1892. (b) Reany, O.; Gunnlaugsson, T.; Parker, D. *J. Chem. Soc., Perkin Trans 2* **2000**, 1819–1831. (c) Hanaoka, K.; Kikuchi, K.; Kojima, H.; Urano, Y.; Nagano, T. *J. Am. Chem. Soc.* **2004**, *126*, 12470–12476.
(10) (a) Bobba, G.; Frias, J. C.; Parker, D. *Chem. Commun.* **2002**, 890–891. (b) Hamblin, J.; Abboyi, N.; Lowe, M. P. *Chem. Commun.* **2005**, 657–659.
(11) Lamture, J. B.; Zhou, Z. H.; Kumar, A. S.; Wensel, T. G. *Inorg. Chem.* **1995**, *34*, 864–869.
(12) Latva, M.; Takalo, H.; Mukkala, V. -M.; Matachescu, C.; Rodríguez-Ubis, J. C.; Kankare, J. *J. Lumin.* **1997**, *75*, 149–169.
(13) Hanaoka, K.; Kikuchi, K.; Kobayashi, S.; Nagano, T. *J. Am. Chem. Soc.* **2007**, *129*, 13502–13509.
(14) (a) Brittain, H. G.; Frederick, S. R.; Martin, R. B. *J. Am. Chem. Soc.* **1976**, *98*, 8255–8260. (b) Bruno, J.; Horrocks, W. D.; Zauher, R. J. *Biochemistry* **1992**, *31*, 7016–7026.
(15) Kumar, K.; Chang, C. A.; Tweedle, M. F. *Inorg. Chem.* **1993**, *32*, 587–593.
(16) Goll, D. E.; Thompson, V. F.; Li, H.; Wei, W.; Cong, J. *Physiol. Rev.* **2003**, *83*, 731–801.
(17) (a) Kinbara, K.; Ishiura, S.; Tomioka, S.; Sorimachi, H.; Jeong, S. Y.; Amano, S.; Kawasaki, H.; Kolmerer, B.; Kimura, S.; Labeit, S.; Suzuki, K. *Biochem. J.* **1998**, *335*, 589596. (b) Lee, M. S.; Kwon, Y. T.; Li, M.; Peng, J.; Friedlander, R. M.; Tsai, L. H. *Nature* **2000**, *405*, 360–364. (c) Mouatt-Prigent, A.; Karlsson, J. O.; Agid, Y.; Hirsch, E. C. *Neuroscience* **1996**, *73*, 979–987.
(18) (a) Sasaki, T.; Kikuchi, T.; Yumoto, N.; Yoshimura, N.; Murachi, T. *J. Biol. Chem.* **1984**, *259*, 12489–12494. (b) Jiang, S. T.; Wang, J. H.; Chang, T.; Chen, C. S. *Anal. Biochem.* **1997**, *244*, 233–238. (c) Mallya, S. K.; Meyer, S.; Bozyczko-Coyne, D.; Siman, R.; Ator, M. A. *Biochem. Biophys. Res. Commun.* **1998**, *248*, 293–296. (d) Mittoo, S.; Sundstrom, L. E.; Bradley, M. *Anal. Biochem.* **2003**, *319*, 234–238. (e) Vanderklish, P. W.; Krushel, L. A.; Holst, B. H.; Gally, J. A.; Crossin, K. L. *Proc. Natl. Acad. Sci. U.S.A.* **2000**, *97*, 2253–2258.

JA800322B